DIFFUSION FROM A LINE SOURCE

Rowland E. Burns

George C. Marshall Space Flight Center
Marshall Space Flight Center, Alabama

November 1973

NASA TECHNICAL MEMORANDUM

1. NASA TM X-64804

2. U/U

(NASA-TM-X-64804) DIFFUSION FROM A LINE SOURCE (NASA) CSCL 04B

N74-17333

Unclas
G3/20 30455

3. NATIONAL AERONAUTICS AND SPACE ADMIN.

4. **DIFFUSION FROM A LINE SOURCE**

By Rowland E. Burns

Aero-Astrodynamics Laboratory

5.

November ~~16~~, ~~1~~973

NASA

George C. Marshall Space Flight Center
Marshall Space Flight Center, Alabama

MSFC - Form 3190 (Rev June 1971)

TECHNICAL REPORT STANDARD TITLE PAGE

1. REPORT NO.	2. GOVERNMENT ACCESSION NO.	3. RECIPIENT'S CATALOG NO.
TMX-64804		

4. TITLE AND SUBTITLE	5. REPORT DATE
DIFFUSION FROM A LINE SOURCE	November 16, 1973
	6. PERFORMING ORGANIZATION CODE
7. AUTHOR(S)	8. PERFORMING ORGANIZATION REPORT #
Rowland E. Burns	
9. PERFORMING ORGANIZATION NAME AND ADDRESS	10. WORK UNIT NO.
George C. Marshall Space Flight Center Marshall Space Flight Center, Alabama 35812	11. CONTRACT OR GRANT NO.
	13. TYPE OF REPORT & PERIOD COVERED
12. SPONSORING AGENCY NAME AND ADDRESS	Technical Memorandum
National Aeronautics and Space Administration Washington, D.C. 20546	14. SPONSORING AGENCY CODE

15. SUPPLEMENTARY NOTES

Prepared by Aero-Astrodynamics Laboratory, Science and Engineering

16. ABSTRACT

The problem with predicting pollutant diffusion from a line source of arbitrary geometry is treated. The concentration at the line source may be arbitrarily varied with time. Special attention is given to the meteorological inputs which act as boundary conditions for the problem, and a mixing layer of arbitrary depth is assumed. Numerical application of the derived theory indicates the combinations of meteorological parameters that may be expected to result in high pollution concentrations.

17. KEY WORDS	18. DISTRIBUTION STATEMENT
	Unclassified-unlimited
	Rowland E. Burns

19. SECURITY CLASSIF. (of this report)	20. SECURITY CLASSIF. (of this page)
Unclassified	Unclassified

ACKNOWLEDGMENT

The author wishes to thank James Alexander, William Ubbens, and Dr. J. Briscoe Stephens who contributed aid in both the programming and theory of this report. Several other friends have already been personally thanked.

TABLE OF CONTENTS

LIST OF ILLUSTRATIONS

LIST OF TABLES

LIST OF SYMBOLS

Latin Symbols	Definition
A	Abbreviation for the product of the integration constants A*, B*, C*, D*, and ϕ_y.
A*	Integration constant
a_p	Coefficients for expansion of the integration constant A
B*	Integration constant
b_p	Coefficients in the expansion of traffic density as a function of time
C*	Integration constant
c_p	Ratio of specific heats of air
$D_0,\ldots,D_6$	Coefficients defined by equation (B-12)
$E_0,\ldots,E_6$	Coefficients defined by equation (B-16)
F	A general function describing the spacial equation of a highway
f	The integral of the z component of the diffusion tensor
G	Buoyancy parameter
g	Acceleration of gravity
H	Effective height of emission of pollutant gasses
h	The integral of the y component of the diffusion tension
I	Integral defined by equation (B-2)
$\hat{i}, \hat{j}, \hat{k}$	Unit Cartesian vectors
i	Unit imaginary symbol
j	Dummy index

LIST OF SYMBOLS (Continued)

Latin Symbols	Definition
$\tilde{K}$	The diffusion tensor
k_x, k_y, k_z	Cartesian components of diffusion tensor
L_i	The length of the "i^{th}" component of a highway
l	Depth of mixing layer
N(t)	Traffic density as a function of time
n	Dummy summation index
P_p	Parameter occurring in the expansion of the integration constant A in equation (50)
p	Dummy summation index
Q	Pollution emission rate
Q_i	Pollution emission rate on segment i of the highway
q_1	Dummy variable in equation (22)
q_2	Dummy variable in equation (22)
S	Total road length
s	Linear translation of the variable r. See equation (B-6)
T	The time dependent portion of the diffusion equation
τ	Temperature
t	Time
T*	A fixed though arbitrary time
u	Mean wind velocity

LIST OF SYMBOLS (Continued)

Latin Symbols	Definition
$\vec{V}$	Vectorial wind
W	The portion of the diffusion equation dependent upon x and z
w	Function of x and t defining the wave front
X	The portion of the diffusion equation dependent upon x
Y	The portion of the diffusion equation dependent upon y
Z	The portion of the diffusion equation dependent upon z
x, y, z	Spacial coordinates
Greek Symbols	
α^2 (or α)	Separation constant in the diffusion equation
β^2	Seperation constant in the diffusion equation
γ^2	Separation constant in the diffusion equation
δ	Constant term in σ_y approximation
ϵ	Slope term in σ_y approximation
ζ	Effective heat released during combustion
η	Expression defined by equation (B-4)
ϑ	$\frac{g}{T}\frac{\partial\theta}{\partial Z}$
Θ	Dummy integration variable
θ	Potential temperature
λ	Parameter in equation (22)

LIST OF SYMBOLS (Concluded)

Greek Symbols	Definition
μ	Expression defined by equation (B-7)
ν	Coefficients in expansion of σ_y and σ_z
ξ	The coefficient of entrainment
ρ	The density of air
σ_y, σ_z	Diffusion parameters in the y and z directions, respectively
Φ	Function defined by equation (34)
ϕ_y	Integration constant
χ	Concentration of diffusing pollutant
ψ	The angle between the wind vector and the sense of the highway
ω	Variable defined by equation (B-10)

Other Notation	
∇	Spacial gradient operator
$'$	Indicates differentiation with respect to the argument
$_0$	(Subscript) Indicates an initial point
$_1$	(Subscript) Indicates an arbitrary though fixed point
*	Indicates a dummy or temporary variable

INTRODUCTION

There has recently been an increased awareness of the fact that pollutants which are normally invisible to the naked eye may pose health hazards. Thus, major efforts have been mounted to control various forms of those hazardous pollutants.

For effective control, effective prediction is necessary. The forecasting of air pollution concentrations presents a very difficult problem of predictibility since many variables influence the concentration of pollutants that are measured at receptor sites. Numerous examples of such variables can be given, such as source strength, source geometry, meteorological influences, chemical reactions involving the pollutants, etc.

The case of automotive pollution emanating from a line source is even more complex than the case of a point source such as a factory. It has been remarked in a recent NASA publication [1] that air pollution models which deal with diffusion from highways and airports are not as refined as those that deal with general urban models. The purpose of this document is to produce a more reasonable model dealing with highways.

The method that will be followed in the derivation of applicable equations is analytic rather than purely numerical. A sophisticated and satisfying treatment could be made via numerical integration of the diffusion equation, but the computational time involved in such a scheme would be quite high. Additionally, numerical integrations on systems of this sort tend toward instability.

The analytical model which is derived here is a compromise between the simple approximations such as occur in Reference 2 and numerical methods.

The following flow chart (Fig. 1) illustrates the structure of the overall model.

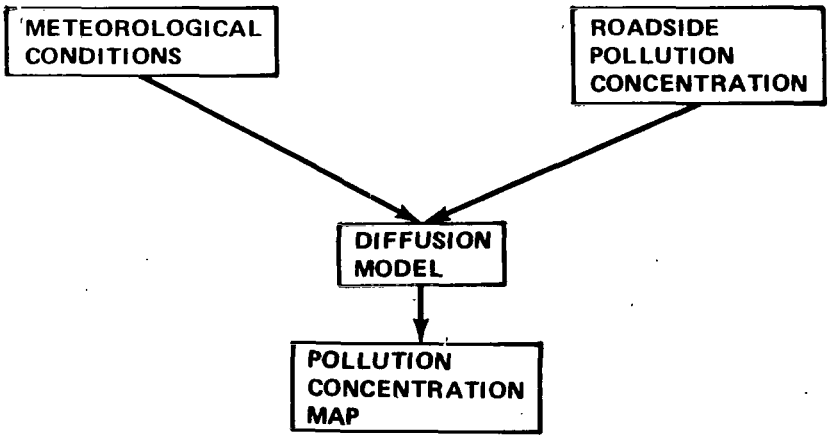

Figure 1. General Flow Chart.

An expanded structure for the block labeled "diffusion model" is required, and we consider inputs to such a model. The basic diffusion model which governs the flow of pollutants is fundamental to the entire discussion. The mechanics of the nondiffusing air is accounted for via meteorological inputs. The source term can be considered to be composed of two components, namely road geometry and traffic density. The important area of chemical reactions of the pollutants will not be considered at this time. The following flow chart (Fig. 2) summarizes the details of the internal structure for the blocks labeled "meteorological conditions" and "roadside pollution concentration."

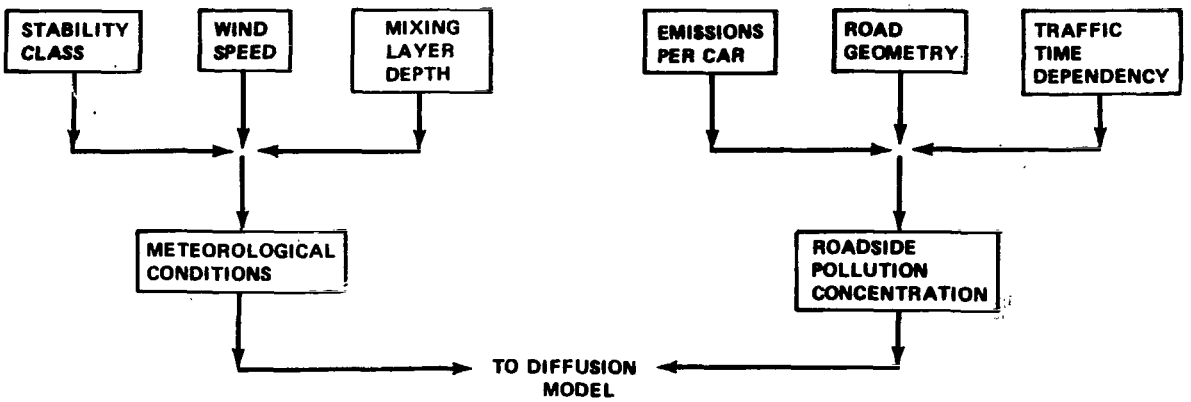

Figure 2. Boundary conditions.

The above outline prescribes an approximate diffusion model which is coupled to both the prevailing meteorological conditions and the (time variable) traffic density. The results of the study provide a rapid method of estimating the concentrations of pollutants from a line source. Based upon the calculations given here, a full scale simulation involving direct numerical integration of the applicable partial differential equations could be undertaken.

In the development, a general separation of the diffusion equation will be accomplished via a product assumption. This requires several subsidiary physical hypotheses, such as thermodynamic independence of the diffusion tensor and averaging of the winds in space and time. The separates chosen are of such form that boundary condition matching is facilitated. The specified separation is followed by boundary condition matching on meteorological parameters and roadside pollution concentration. Finally, the varying road geometry is taken into account by either numerical integration or segmentation or an approximate analytic method. The theory is applied to yield parametric results and the numerical behavior of the equations is demonstrated.

THE DIFFUSION EQUATION

The standard equation for a diffusing gas [2] is

$$\frac{\partial \chi}{\partial t} + \vec{V} \cdot \nabla \chi = \nabla \cdot (\tilde{K} \cdot \nabla \chi) \quad , \tag{1}$$

where

χ is the concentration of the diffusing gas, a function of both time and space variables,

$\vec{V}$ is the vectorial wind velocity, which will be taken as an average value,

$\tilde{K}$ is the diffusion tensor,

t is the time, and

∇ is the spacial gradient operator.

It is possible, via a rotation to diagonalize $\tilde{K}$ so that

$$\tilde{K} = k_x \hat{i}\hat{i} + k_y \hat{j}\hat{j} + k_z \hat{k}\hat{k} \quad , \tag{2}$$

where $\hat{i}$, $\hat{j}$, and $\hat{k}$ represent cartesian unit vectors. The components of $\tilde{K}$ (k_x, k_y, and k_z) represent the so-called eddy diffusivities, and are functions of the down-wind distance. The physical basis of a variable diffusivity is that the pollution cloud spreads as it leaves the road and interacts with eddies which are of the scale of the cloud. Thus, taking k_x, k_y, and k_z as constants is not physically satisfactory. By Reference 2, we take

$$\begin{aligned} k_x &\equiv 0 \text{ (by superposition)}, \\ k_y &= k_y(x) \quad , \text{ and} \\ k_z &= k_z(x) \quad . \end{aligned} \tag{3}$$

Assuming that the vector velocity, $\vec{V}$, lies along the x axis yields

$$\vec{V} = \bar{u}\,\hat{i} \quad , \tag{4}$$

where $\bar{u} = |\vec{V}|$. (The case where $\vec{V}$ does not lie along the x axis will be considered at a later time.)

Inserting (2), (3), and (4) into (1) yields

$$\frac{\partial \chi}{\partial t} + \bar{u}\frac{\partial \chi}{\partial x} = k_y(x)\frac{\partial^2 \chi}{\partial y^2} + k_z(x)\frac{\partial^2 \chi}{\partial z^2} \quad . \tag{5}$$

This equation is at least partially separable. Assume that

$$\chi = T(t)\,Y(y)\,W(x,z) \quad ; \tag{6}$$

so that (5) becomes

$$\frac{T'}{T} + \frac{\bar{u}}{w}\frac{\partial W}{\partial x} = k_y(x)\frac{Y''}{Y} + \frac{k_z(x)}{w}\frac{\partial^2 W}{\partial z^2} \quad , \tag{7}$$

where the prime (′) denotes differentiation with respect to the argument. Isolation of the only component dependent upon T yields

$$\frac{T'}{T} = -\alpha^2 = k_y(x)\frac{Y''}{Y} + \frac{k_z(x)}{w}\frac{\partial^2 W}{\partial z^2} - \frac{\bar{u}}{w}\frac{\partial W}{\partial x} \quad , \tag{8}$$

where α^2 is a separation constant of unknown properties. Thus

$$T = A^* e^{-\alpha^2 t} \quad , \tag{9}$$

where A^* is an integration constant. Isolating the Y component of (8) yields

$$\frac{Y''}{Y} = \frac{1}{k_y(x)}\left[-\alpha^2 - \frac{k_z(x)}{w}\frac{\partial^2 w}{\partial z^2} + \frac{\bar{u}}{w}\frac{\partial W}{\partial x}\right] = -\beta^2 \quad , \tag{10}$$

where $-\beta^2$ is a second separation constant. Then

$$Y = B^* \cos(\beta y + \phi_y) \tag{11}$$

and B^*, ϕ_y are integration constants.

The residue of (10) may now be written as

$$k_z(x)\frac{\partial^2 w}{\partial z^2} - \bar{u}\frac{\partial W}{\partial x} = \left[\alpha^2 - \beta^2 k_y(x)\right] W \quad . \tag{12}$$

It would be physically reasonable to require that $\bar{u} = \bar{u}(z)$ and proceed with the integration of (12) on that basis. A difficulty arises in that no method of integration has been found for this equation with variable k_z and k_y unless $\bar{u}$ is assumed to be constant. This is, mathematically, why most authors always use average values of $\bar{u}$. To obtain an initial separation it was necessary to assume that $\bar{u}$ was averaged in time and along y. It is now necessary to assume that $\bar{u}$ is averaged in z as well. In Reference 3 it is stated that one almost never has enough data to establish the dependency of $\bar{u}$ on z in any case. Thus, we assume that

$$W(x,z) = X(x)\,Z(z) \quad , \tag{13}$$

so that (12) becomes

$$\frac{Z''}{Z} = \frac{1}{k_z(x)}\left[-\alpha^2 + \bar{u}\frac{X'}{X} + \beta^2 k_y(x)\right] = -\gamma^2 \quad . \tag{14}$$

The total differential equation for Z is, then,

$$Z'' + \gamma^2 Z = 0 \tag{15}$$

The solution of equation (15) could be written exactly as (11) was written as a solution for (10). But it is convenient to choose a special form with an eye toward matching boundary conditions. Thus we write,

$$Z = C^* \Bigg\{ \cos \gamma(z - H) + \cos \gamma(z + H) + \sum_{n=1}^{\infty} \Big[\cos \gamma(z - H - 2nl) + \cos \gamma(z - H + 2nl) + \cos \gamma(z + H - 2nl) + \cos \gamma(z + H + 2nl) \Big] \Bigg\} . \tag{16}$$

(The parameters H and l, arbitrarily introduced into (16), have physical significance. It will later be shown that l is the depth of a mixing layer, i.e., an upper lid which is not penetrated by the pollution cloud. H is the effective height of emission of the gases which arise due to the fact that such gases are normally warmer than the ambient air.)

We also have, from (14),

$$X' = \frac{1}{\bar{u}} \Big[- \gamma^2 k_z(x) + \alpha^2 - \beta^2 k_y(x) \Big] X \quad , \tag{17}$$

which has the solution

$$X = D^* \exp \left[- \frac{\gamma^2}{\bar{u}} \int_{x_o}^{x} k_z(x)\, dx - \frac{\beta^2}{u} \int_{x_o}^{x} k_y(x)\, dx + \frac{\alpha^2}{\bar{u}} (x - x_o) \right] , \tag{18}$$

where x_o is an arbitrary reference length. (Later x_o will be chosen to be the half-width of the road.)

For algebraic convenience, we define

$$f(x) = \int_{x_o}^{x} k_z(x)\,dx \quad , \quad \text{and}$$

$$h(x) = \int_{x_o}^{x} k_y(x)\,dx \quad . \tag{19}$$

Using (19) in (18) and the resultant equation, along with (16), (13), (11), and (9) in (6) gives

$$\chi = A^* B^* C^* D^* e^{-\alpha^2\left(t - \frac{x - x_o}{\bar{u}}\right)} e^{-\frac{\gamma^2 f(x)}{\bar{u}}} e^{-\frac{\beta^2 h(x)}{u}} \cos(\beta y + \phi_y) \left\{\cos \gamma(z - H)\right.$$

$$+ \cos \gamma(z + H) + \sum_{n=1}^{\infty} \left[\cos \gamma(z - H - 2nl) + \cos \gamma(z - H + 2nl)\right.$$

$$\left.\left. + \cos \gamma(z + H - 2nl) + \cos \gamma(z + H + 2nl)\right]\right\} \quad , \tag{20}$$

which is the formal separated solution of (6).

BOUNDARY CONDITION MATCHING

Since the separated equation is degenerate in the (t,x) pair, it is obvious that boundary conditions can be matched only on z, y, and (t,x). We begin with z. The eigenvalues, γ, form a continuous spectrum so we can write

$$\chi = XTY \int_{-\infty}^{\infty} e^{-\frac{\gamma^2 f(x)}{\bar{u}}} \left\{\cos \gamma(z - H) + \cos \gamma(z + H) + \sum_{n=1}^{\infty} \left[\cos \gamma(z - H - 2nl)\right.\right.$$

$$\left.\left. + \cos \gamma(z - H + 2nl) + \cos \gamma(z + H + 2nl) + \cos \gamma(z + H - 2nl)\right]\right\} d\gamma \tag{21}$$

From Reference 5, eq. 3.896 we have

$$\int_{-\infty}^{\infty} e^{-q_1^2 x^2} \cos q_2 (x + \lambda)\, dx = \frac{\sqrt{\pi}}{q_1} e^{-\frac{q_2^2}{4q_1^2}} \cos q_2 \lambda \quad . \tag{22}$$

Identification of variables between (22) and (21) yields

$$\int_{-\infty}^{\infty} e^{-\frac{\gamma^2 f(x)}{\bar{u}}} \cos \gamma(z \pm H \pm 2nl)\, d\gamma = \sqrt{\frac{\pi\bar{u}}{f}}\, e^{-\frac{(z \pm H \pm 2nl)^2\, \bar{u}}{4f(x)}} \quad . \tag{23}$$

Similarly, (21) can be written as

$$\chi = XTZ \int_{-\infty}^{\infty} e^{-\frac{\beta^2 h(x)}{\bar{u}}} \cos(\beta y + \phi_y)\, dy = \sqrt{\frac{\pi\bar{u}}{h}}\, e^{-\frac{y^2\bar{u}}{4h}} \cos \phi_y \quad . \tag{24}$$

Thus, including all possible values of β and γ shows that (20) may be written, with $A = A^* B^* C^* D^* \cos \phi_y$, as

$$\chi = \frac{A\pi\bar{u}}{\sqrt{fh}}\, e^{-\alpha^2\left(t - \frac{x - x_o}{\bar{u}}\right)} e^{-\frac{y^2\bar{u}}{4h}} \left\{ e^{-\frac{\bar{u}}{4f}(z - H)^2} + e^{-\frac{\bar{u}}{4f}(z + H)^2} \right.$$

$$+ \sum_{n=1}^{\infty} \left[e^{-\frac{\bar{u}}{4f}(z - H - 2nl)^2} + e^{-\frac{\bar{u}}{4f}(z + H + 2nl)^2} + e^{-\frac{\bar{u}}{4f}(z + H - 2nl)^2} \right.$$

$$\left. \left. + e^{-\frac{\bar{u}}{4f}(z - H + 2nl)^2} \right] \right\} \quad . \tag{25}$$

It is now convenient to modify out notation slightly to be in agreement with the standard literature. The quantities u/f and u/h are not generally tabulated. Instead we find, as in [3], direct tabulations of the quantities σ_y and σ_z. Physically σ_y and σ_z are quantities such that ~ 97 percent of the mass of the pollutants are contained in a cloud of radius 2.15σ. Mathematically,

$$\sigma_y = + \sqrt{\frac{2h}{\bar{u}}} \quad , \text{ and}$$

$$\sigma_z = + \sqrt{\frac{2f}{\bar{u}}} \tag{26}$$

are given. Inserting σ_y and σ_z in (25) gives the more compact form

$$\chi = \frac{2A\pi}{\sigma_y \sigma_z} e^{-\alpha^2 \left(t - \frac{x-x_o}{\bar{u}}\right)} e^{-\frac{1}{2}\left(\frac{y}{\sigma_y}\right)^2} \left\{ e^{-\frac{1}{2}\frac{(z-H)^2}{\sigma_z^2}} + e^{-\frac{1}{2}\frac{(z+H)^2}{\sigma_z^2}} \right.$$

$$+ \sum_{n=1}^{\infty} \left[e^{-\frac{(z-H-2nl)^2}{2\sigma_z^2}} + e^{-\frac{(z-H+2nl)^2}{2\sigma_z^2}} + e^{-\frac{(z+H+2nl)^2}{2\sigma_z^2}} \right.$$

$$\left. \left. + e^{-\frac{(z+H-2nl)^2}{2\sigma_z^2}} \right] \right\} \tag{27}$$

It is now possible to illustrate an important set of properties of the "Z" portion of (27). We have

$$\frac{\partial Z}{\partial z} = -\frac{1}{\sigma_z^2} \left\{ (z-h)\, e^{-\frac{1}{2}\frac{(z-H)^2}{\sigma_z^2}} + (z+H)\, e^{-\frac{1}{2}\frac{(z+H)^2}{\sigma_z^2}} \right.$$

$$+ \sum_{n=1}^{\infty} \left[(z-H-2nl)\, e^{-\frac{(z-H-2nl)^2}{2\sigma_z^2}} + (z-H+2nl)\, e^{-\frac{(z-H+2nl)^2}{2\sigma_z^2}} \right.$$

$$\left. \left. + (z+H+2nl)\, e^{-\frac{(z+H+2nl)^2}{2\sigma_z^2}} + (z+H-2nl)\, e^{-\frac{(z+H-2nl)^2}{2\sigma_z^2}} \right] \right\} \tag{28}$$

Notice that

$$\left.\frac{\partial Z}{\partial z}\right|_{z=0} = 0 \quad . \tag{29}$$

Similarly, an expansion of the series shows that

$$\left.\frac{\partial Z}{\partial z}\right|_{z=l} = 0 \quad . \tag{30}$$

From [4], equations (29) and (30) ensure that the ground and a mixing layer of arbitrary depth, 1, are impervious to pollution transfer.

Also, if we allow l to become large in (27) we find that Z can be written as

$$Z = XTY\left[e^{-\frac{1}{2}\frac{(z-H)^2}{\sigma_z^2}} + e^{-\frac{1}{2}\frac{(z+H)^2}{\sigma_z^2}}\right] ,$$

which corresponds to the physically unrealistic case of a superadiabatic atmosphere of infinite depth.

The next modification of (27) to meet the specific model we wish to consider involves the fact that (27) represents a point source, not a distributed source such as a road. The following figure is applicable.

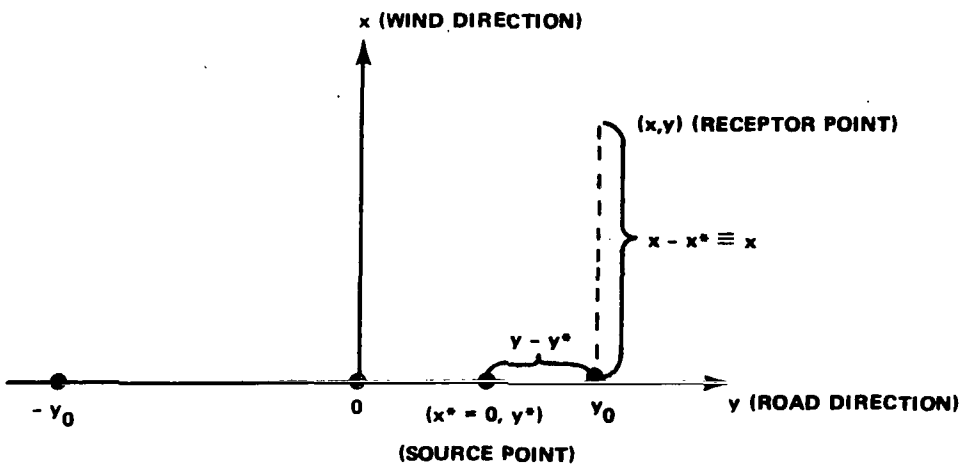

Figure 3. Distributed Source Geometry.

($-y_o$, y_o are, respectively, the Eastern and Western terminus point of the road segment under consideration.)

We have, from (27),

$$\chi = XTZ\, e^{-\frac{1}{2}\frac{y^2}{\sigma_y^2}}$$

for a point source at (0,0). But for a point source at (0,y*) of strength Qdy* per unit distance, we must have

$$d\chi = QXTZ\, e^{-\frac{(y - y^*)^2}{2\sigma_y^2}}\, dy^*$$

or

$$\chi = QXTZ \int_{-y_o}^{y_o} e^{-\frac{(y - y^*)^2}{2\sigma_y^2}}\, dy^*$$

Setting

$$\Theta = \frac{(y^* - y)}{\sqrt{2}\sigma_y}$$

we have

$$d\Theta = \frac{dy^*}{\sqrt{2}\sigma_y}$$

And when

$$y^* = \pm y_o \quad ,$$

we must have

$$\Theta = \pm \frac{(y_o \mp y)}{\sqrt{2}\,\sigma_y}$$

Thus,

$$\chi = \sqrt{2}\,\sigma_y\,QXTZ \int_{-\frac{(y_o + y)}{\sqrt{2}\,\sigma_y}}^{\frac{y_o - y}{\sqrt{2}\,\sigma_y}} e^{-\Theta^2}\,d\Theta = \sqrt{\pi}\,\sigma_y\,QXTZ \left\{ \operatorname{erf}\left[\frac{y_o + y}{\sqrt{2}\,\sigma_y}\right] + \operatorname{erf}\left[\frac{y_o - y}{\sqrt{2}\,\sigma_y}\right] \right\} \tag{31}$$

or

$$\chi = \frac{2\,A(\pi)^{3/2}\,Q}{\sigma_z}\, e^{-\alpha^2\left(t - \frac{x - x_o}{\bar{u}}\right)} \left\{ \operatorname{erf}\left[\frac{(y_o + y)}{\sqrt{2}\,\sigma_y}\right] + \operatorname{erf}\left[\frac{y_o - y}{\sqrt{2}\,\sigma_y}\right] \right\} \left\{ e^{-\frac{1}{2}\frac{(z - H)^2}{\sigma_z^2}} + e^{-\frac{1}{2}\frac{(z + H)^2}{\sigma_z^2}} + \sum_{n=1}^{\infty} \left[e^{-\frac{(z - H - 2nl)^2}{2\sigma_z^2}} + e^{-\frac{(z - H + 2nl)^2}{2\sigma_z^2}} + e^{-\frac{(z + H - 2nl)^2}{2\sigma_z^2}} + e^{-\frac{(z + H + 2nl)^2}{2\sigma_z^2}} \right] \right\} \tag{32}$$

Equation (32) is not yet normalized and does not yet account for traffic density. There would be a certain elegance involved in a car-by-car trace which gives rise to a complicated coupling between y and t, but this is hardly necessary. We will, instead, simply assume that the travel time of any car on the road is short compared to the time over which the pollution cloud is observed. Equivalently, we shall assume that the variation of traffic at the center point of the road represents the variation of traffic along the entire road, and match our boundary condition in time at this point.

In order to match the traffic density boundary condition, we shall make use of the the remaining separation parameter (α) and the "constant" A. Note that no violation of equation (1) results if we assume that A is a function of α. Furthermore, in order to obtain a normalized function we evaluate χ as the point $(x_o, 0, 0, t)$ as

$$\chi(x_o,0,0,t) = \frac{8\,A(\alpha)(\pi)^{3/2}\,Q}{\sigma_z(x_o)}\; e^{-\alpha^2 t}\left(\operatorname{erf}\frac{y_o}{\sqrt{2}\,\sigma_y(x_o)}\right)\left\{ e^{-\frac{1}{2}\frac{H^2}{\sigma_z^2}} + \sum_{n=1}^{\infty}\left[e^{-\frac{(H+2nl)^2}{2\sigma_z^2}} + e^{-\frac{(H-2nl)^2}{2\sigma_z^2}}\right]\right\} . \tag{33}$$

For algebraic convenience, we label

$$\Phi = \frac{8(\pi)^{3/2}Q}{\sigma_z(x_o)}\;\operatorname{erf}\left[\frac{y_o}{\sqrt{2}\,\sigma_y(x_o)}\right]\left\{ e^{-\frac{1}{2}\frac{H^2}{\sigma_y^2}} + \sum_{n=1}^{\infty}\left[e^{-\frac{(H+2nl)^2}{2\sigma_z^2}} + e^{-\frac{(H-2nl)^2}{2\sigma_z^2}}\right]\right\} \tag{34}$$

so that (33) becomes

$$\chi(x_o,0,0,t) = \Phi\, A(\alpha)\, e^{-\alpha^2 t} . \tag{35}$$

Accounting for all possible values of α gives

$$\chi(x_o,0,0,t) = \Phi \int^{\infty} A(\alpha)\, e^{-\alpha^2 t}\, d\alpha \quad , \tag{36}$$

where the lower limit is deliberately unspecified.

We wish now to assert that at $(x_o,0,0,t)$, the pollution density at roadside is given by

$$\chi(x_o,0,0,t) = Q\, N(t) \quad , \tag{37}$$

where Q is the emission per car per unit distance and N(t) is the number of cars per unit time. Thus given N(t) we wish to solve for $A(\alpha)$ such that

$$Q\, N(t) = \Phi \int^{\infty} A(\alpha)\, e^{-\alpha^2 t}\, d\alpha \quad . \tag{38}$$

where N(t) may be expanded into an arbitrary series which is subject only to well behaved numerical behavior properties. (The possibility that N(t) could be represented by a single, simple, analytic function is so remote as to be negligible.)

Three cases will be considered. In the first case we shall deal directly with α^2 and the range of integration will be $(-\infty,\infty)$. Secondly, if we assume that α can be written in place of α^2, then $A(\alpha)$ becomes the inverse Laplacian of $Q\,N(t)/\Phi$. The integration range, in that case, is $(0,\infty)$. Finally, if we assume α to be a purely imaginary number, which implies that $A(\alpha)$ is the inverse Fourier transform of $Q\,N(t)/\Phi$.

For the first possibility, assume that

$$A(\alpha) = \sum_{p=1}^{n} a_p (\alpha^2)^p \quad , \tag{39}$$

so that (38) yields

$$Q\, N(t) = \Phi \int_{-\infty}^{\infty} \sum_{p=1}^{M} a_p\, \alpha^{2p}\, e^{-\alpha^2 t}\, d\alpha = \Phi \sum_{p=1}^{M} \frac{(2p-1)!!\sqrt{\pi}}{2^p\, t^{p+\frac{1}{2}}}\, a_p \tag{40}$$

(Reference 5, eq. 3.461). Since $N(t)$ is an empirical function, assume that it may be presented as

$$N(t) = \sum_{p=1}^{M} \frac{b_p}{t^{p+1/2}} \quad . \tag{41}$$

Then we must have

$$a_p = \frac{2^n b_p}{(2p-1)!!\sqrt{\pi}\ \Phi} \quad , \tag{42}$$

so that

$$A(\alpha) = \sum_{p=1}^{M} \frac{2^p b_p \alpha^{2p}}{(2p-1)!!\sqrt{\pi}\ \Phi} \quad . \tag{43}$$

Finally, the expression for χ, equation (32), can be written as

$$\chi = \left(\frac{2(\pi)^{3/2} Q}{\sigma_z}\right)\left(\frac{Q}{\Phi}\right)\int_{-\infty}^{\infty} \sum_{p=1}^{M} \frac{2^p b_p \alpha^{2p}}{(2p-1)!!\sqrt{\pi}}\ e^{-\alpha^2\left(t - \frac{x - x_o}{\bar{u}}\right)}\, d\alpha$$

$$= \left(\frac{2\pi Q}{\sigma_z}\right)\left(\frac{Q}{\Phi}\right) YZ \sum_{p=1}^{M} \frac{b_p}{\left(t - \frac{x - x_o}{\bar{u}}\right)^{p+1/2}} \tag{44}$$

We next assume that α may have only positive values and choose

$$A(\alpha) = \sum_{p=1}^{M} a_p \cos p\alpha \quad , \tag{45}$$

so that

$$\chi(x_o,0,0,t) = Q\,N(t) = \Phi \int_o^\infty \sum_{p=1}^{M} a_p \cos p\alpha\, e^{-\alpha t}\, d\alpha = \Phi \sum_{p=1}^{M} \frac{a_p\, t}{t^2 + p^2} \qquad (46)$$

Assuming that χ is readily fit as

$$\chi = Q \sum_{p=1}^{M} \frac{b_p\, t}{t^2 + p^2} \qquad (47)$$

we identify

$$a_p = \frac{Q\, b_p}{\Phi} \quad ; \qquad (48)$$

so that

$$\chi = \left[\frac{2\,(\pi)^{3/2}\,Q}{\sigma_z}\right]\left(\frac{Q}{\Phi}\right) YZ \int_o^\infty \sum_{p=1}^{M} b_p \cos p\alpha\, e^{-\alpha\left(t - \frac{x - x_o}{\bar{u}}\right)}\, d\alpha$$

$$= \left(\frac{2\,(\pi)^{3/2}\,Q}{\sigma_z}\right)\left(\frac{Q}{\Phi}\right) YZ \sum_{p=1}^{M} \frac{b_p\left(t - \frac{x - x_o}{u}\right)}{\left(t - \frac{x - x_o}{u}\right)^2 + p^2} \qquad (49)$$

Finally, we choose a purely imaginary separation constant and define

$$A(\alpha) = \sum_{p=1}^{M} \frac{a_p}{\sqrt{2\,P_p}} \sin\left(\frac{\alpha^2}{4\,P_p} + \frac{\pi}{4}\right) \qquad (50)$$

Then

$$\chi(x_o,0,0,t) = Q\,N(t) = \Phi \int_{-\infty}^{\infty} \sum_{p=1}^{M} \frac{a_p}{\sqrt{2\,P_p}} \sin\left(\frac{\alpha^2}{4\,P_p} + \frac{\pi}{4}\right) e^{-i\alpha t}$$

$$= \Phi \sum_{p=1}^{M} a_p \sin\,(P_p\,t^2) \quad . \tag{51}$$

Thus, if we can write, conveniently,

$$N(t) = \sum_{p=1}^{M} b_p \sin\,(P_p\,t^2) \quad , \tag{52}$$

we must have

$$a_p = \frac{Q\,b_p}{\Phi} \quad . \tag{53}$$

Finally,

$$\chi = \left[\frac{2\,(\pi)^{3/2}\,Q}{\sigma_z}\right]\left(\frac{Q}{\Phi}\right) YZ \int_{-\infty}^{\infty} \sum_{p=1}^{M} \frac{b_p}{\sqrt{2\,P_p}} \sin\left(\frac{\alpha^2}{4\,P_p} + \frac{\pi}{4}\right) e^{-i\alpha\left(t - \frac{x - x_o}{\bar{u}}\right)} d\alpha$$

$$= \left(\frac{2\,(\pi)^{3/2}\,Q}{\sigma_z}\right)\left(\frac{Q}{\Phi}\right) YZ \sum_{p=1}^{M} b_p \sin P_p \left(t - \frac{x - x_o}{\bar{u}}\right)^2 \tag{54}$$

The choice of equation (44), (49), or (54) is arbitrary from the theoretical point of view. Numerically, however, the behavior of the three equations differs markedly. Whichever of these best fits the traffic pattern should be used.

Equation (54) may be fully written as

$$\chi(x,y,z,t) = \frac{Q}{4}\frac{\sigma_z(x_o)}{\sigma_z(x)}\frac{\left[\operatorname{erf}\left(\frac{y_o+y}{\sqrt{2}\,\sigma_y}\right)+\operatorname{erf}\left(\frac{y_o-y}{\sqrt{2}\,\sigma_y}\right)\right]}{\operatorname{erf}\frac{y_o}{\sqrt{2}\,\sigma_y(x_o)}}\sum_{p=1}^{M} b_p \sin P_p\left(t-\frac{x-x_o}{\bar{u}}\right)^2$$

$$\frac{\left\{e^{-\frac{(z-H)^2}{2\sigma_z^2}}+e^{-\frac{(z+H)^2}{2\sigma_z^2}}+\sum_{n=1}^{\infty}\left[e^{-\frac{(z-H-2nl)^2}{2\sigma_z^2}}+e^{-\frac{(z-H+2nl)^2}{2\sigma_z^2}}+e^{-\frac{(z+H+2nl)^2}{2\sigma_z^2}}+e^{-\frac{(z+H-2nl)^2}{2\sigma_z^2}}\right]\right\}}{\left[e^{-\frac{H^2}{2\sigma_z(x_o)^2}}+\sum_{n=1}^{\infty}\left(e^{-\frac{(H+2nl)^2}{2\sigma_z(x_o)^2}}+e^{-\frac{(H-2nl)^2}{2\sigma_z(x_o)^2}}\right)\right]} \qquad (55)$$

Equations (44), (49), and (54) represent three possible solutions out of an infinite number of choices which could be made for $A(\alpha)$, and they are convenient from certain points of view. An additional purely numerical scheme is also worth considering. These equations all share the property that they are degenerate in the variables t and x. This is a direct result of the assumption that $k_x(x)$ vanishes. Set, for convenience

$$w(t,x) = t - \frac{x - x_o}{\bar{u}} \geqslant 0 \quad ,$$

and consider a coordinate $x_1 > x_o$, and a time $t = t_1$. Then

$$\exists t^* : (t^* < t) \wedge \left[w(t^*, x_o) = w(t_1, x_1) \right] \quad ,$$

where we can explicitly define

$$t^* = t - \frac{x_1 - x_o}{\bar{u}} \quad .$$

This represents a retarded time wave. The practical result of this observation is that if we define the traffic density as a dense function (perhaps even via interpolation), then the representation of the traffic via calculation of polynomial coefficients becomes unnecessary.

ROAD GEOMETRY

It was earlier stated that we would temporarily assume that the road was perfectly straight and that the vectorial wind was orthogonal to the road. In practice, of course, roads are rarely straight and this fact must be included in the theory which has been presented.

Several methods of approach suggest themselves. We could, for example, curve fit a polynomial between the x and y coordinates of the road, obtaining a relationship such as

$$y^* = F(x^*) \tag{56}$$

and integrate an equation similar to (31), after replacing x by $x - x^*$ and y by $y - y^*$. Such a process is possible, but would most likely prove unsatisfactory due to the complexities of curve fits within curve fits and the machine time required for complicated numerical integrals.

A slightly modified approach would be to break the road into linear segments and not assume that the wind is orthogonal to the road. That is, assume that (56) is a linear relationship via

$$y^* = x^* \tan \psi \quad , \tag{57}$$

where ψ is the angle between the y axis and the road (Fig. 4).

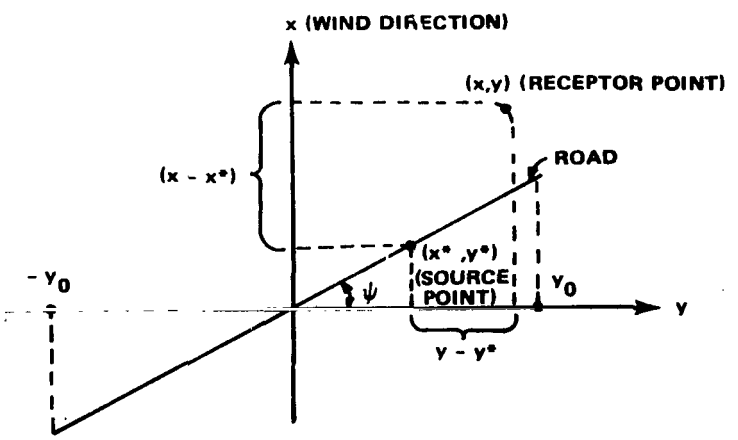

Figure 4. Nonorthogonal Wind Geometry.

Thus, (55) would be written as

$$\chi(x,y,z,t) = \frac{Q}{4}\,\sigma_z(x_o)\,\sigma_y(x_o)\int_{-y_o\tan\psi}^{y_o\tan\psi}\left(e^{-\frac{(y-x^*\tan\psi)^2}{2\sigma_y^2(x-x^*)}}\sum_{p=1}^{M} b_p \sin P_p\left[t-\frac{x-x^*-x_o}{\bar{u}}\right]^2\right.$$

$$\cdot\left[\frac{1}{\sigma_y(x-x^*)\,\sigma_z(x-x^*)}\right]\left\{e^{-\frac{(z-H)^2}{2\sigma_z^2(x-x^*)}} + e^{-\frac{(z+H)^2}{2\sigma_z^2(x-x^*)}}\right.$$

$$+\sum_{n=1}^{\infty}\left[e^{-\frac{(z-H-2nl)^2}{2\sigma_z^2(x-x^*)}} + e^{-\frac{(z-H+2nl)^2}{2\sigma_z^2(x-x^*)}} + e^{-\frac{(z+H+2nl)^2}{2\sigma_z^2(x-x^*)}}\right.$$

$$\left.\left.\left.+ e^{-\frac{(z+H-2nl)^2}{2\sigma_z^2(x-x^*)}}\right]\right\}\right) dx^*$$

which is a none too pleasant integral.*

A third possibility, an approximation that offers some hope of numerical application is as follows. Consider a road of arbitrary geometry. Segment the road into a large number of individual straight segments and apply, say, (55) to each of the pieces (Fig. 5). Subsequently, the segments are added linearly to obtain the total air pollution. Graphically we have:

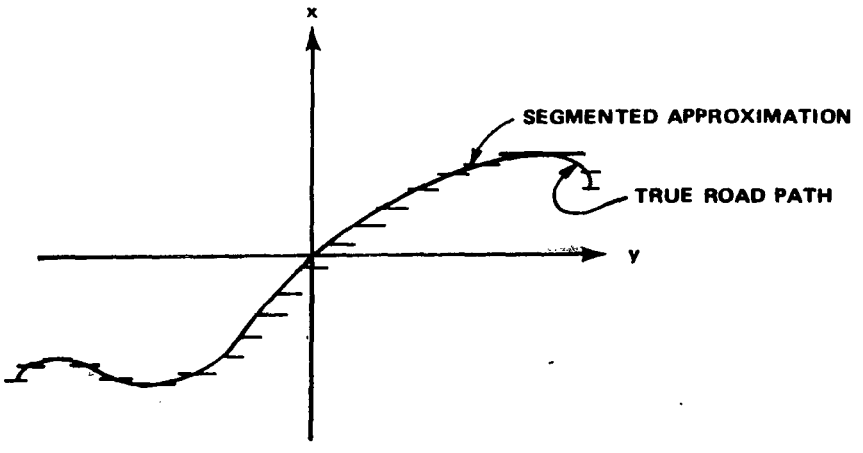

Figure 5. Nonlinear Source Geometry.

* An analytical approximation to this integral is developed in Appendix B.

To rewrite (55) in such a way as to account for such segmentation, assume that the road is broken into k segments, each of length 2L (Fig. 6). Label a generic segment by the subscript i, and assume that it is centered at the point x_i, y_i.

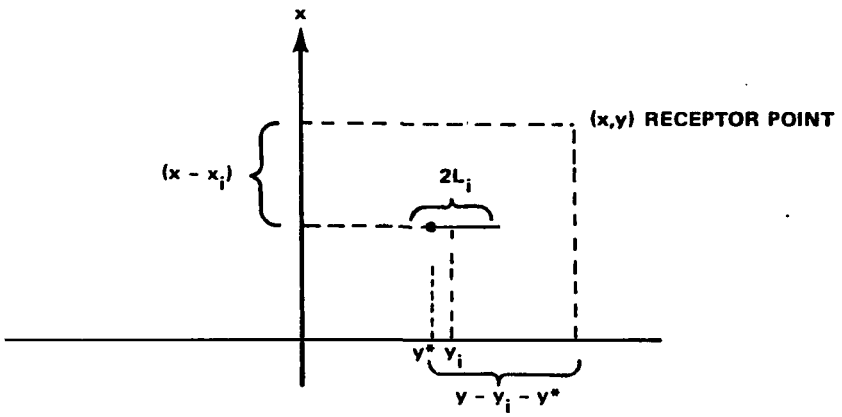

Figure 6. Linearized Source Approximation.

If we assume an imaginary separation constant, then the new form is available directly from (55). Thus we have an accounting for all segments,

$$x = \sum_{i=1}^{k} \left(\frac{Q_i}{2} \frac{\sigma_z(x_o)}{\sigma_z(x - x_i)} \left[\frac{\operatorname{erf} \frac{(y - y_i - L_i)}{\sqrt{2}\,\sigma_y(x - x_i)} + \operatorname{erf} \frac{(y - y_i + L_i)}{\sqrt{2}\,\sigma_y(x - x_i)}}{\operatorname{erf}\left(\frac{L_i - y_i}{\sqrt{2}\,\sigma_y(x_o)}\right) - \operatorname{erf}\left(\frac{L_i + y_i}{\sqrt{2}\,\sigma_y(x_o)}\right)} \right] \sum_{p=1}^{k} b_p \sin P_p \left(t - \frac{x - x_i - x_o}{\bar{u}} \right)^2 \right.$$

$$\left. \left\{ e^{-\frac{(z - H)^2}{2\sigma_z^2(x - x_i)}} + e^{-\frac{(z + H)^2}{2\sigma_z^2(x - x_i)}} + \sum_{n=1}^{\infty} \left[e^{-\frac{(z + H + 2nl)^2}{2\sigma_z^2(x - x_i)}} + e^{-\frac{(z + H - 2nl)^2}{2\sigma_z^2(x - x_i)}} + e^{-\frac{(z - H + 2nl)^2}{2\sigma_z^2(x - x_i)}} + e^{-\frac{(z - H - 2nl)^2}{2\sigma_z^2(x - x_i)}} \right] \right\} \right.$$

$$\left. \left\{ e^{-\frac{(H^2)}{2\sigma_z^2(x_o)}} + \sum_{n=1}^{\infty} \left[e^{-\frac{(H + 2nl)^2}{2\sigma_z^2(x_o)}} + e^{-\frac{(H - 2nl)^2}{2\sigma_z^2(x_o)}} \right] \right\} \right) \tag{58}$$

Since the true road length, S, will vary from the segmented length, $2\sum_{i=1}^{k} L_i$, we ensure conservation of pollution by scaling

$$Q_i = \frac{QS}{2 \sum_{i=1}^{k} L_i} .$$

Furthermore, Q_i may be varied along the route to account for high pollution points such as interchanges.

ROADSIDE POLLUTION CONCENTRATION

Using equation (58) as a specific example, it is apparent that the Q_i's are not yet specified. Other parameters, such as x_o, x_i, σ_x, σ_y, etc. are available from other design estimates or tabulated data, but the Q_i's require further development.

To begin the discussion, the emission rates in mass per unit length of travel from automobiles have been published in Reference 6. (These emission rates vary according to load.) Assume that under given conditions automobiles emit an average of Q_i^* grams per meter per vehicle. The only other dimensional quantity in equation (58) is the traffic density, N(t), which is measured in vehicles per second. Thus, equation (58) reads, dimensionally,

$$[\chi] = [Q]\,[N]$$

or

$$\frac{\text{Mass}}{\text{Length}^3} = [Q]\ \frac{\text{veh}}{\text{Time}}$$

where: M is mass, L is length, and τ is time. Assume a volume over which the emissions are stabilized. This volume is of height H, length L and expands in a direction perpendicular to the road at a rate $\bar{u}$. The volume described is given by $L_i H\bar{u}$; where, as before, L_i is the length of the road which is considered.

Thus,

$$Q_i = \frac{L_i Q_i^*}{L_i H\bar{u}} = \frac{Q_i^*}{H\bar{u}}$$

so that

$$[Q_i] = \frac{[Q_i^*]}{[H]\,[\bar{u}]} = \frac{\text{Mass}\cdot\text{Time}}{\text{Length}^3 \cdot \text{Vehicles}}$$

Obviously

$$[\chi] = \frac{\text{Mass} \cdot \text{Time}}{\text{Length}^3 \cdot \text{Vehicles}} \cdot \frac{\text{Vehicles}}{\text{Time}} = \frac{\text{Mass}}{\text{Length}^3}$$

INPUT VARIABLES

We shall now apply the theory which has been developed to sample data cases. The program used in the generation of this data is documented in Appendix A.

Perhaps one of the most important sets of parameters given in the preceding are the diffusion coefficients σ_y and σ_z. These quantities are fairly complicated functions of the distance from the source, x, and the meteorological category. From Reference 7, we have the following tables.

TABLE 1. DIFFUSION COEFFICIENT σ_y, M

Distance From Source, Meters	Meteorological Categories					
	A	B	C	D	E	F
10^2	22	16	12	8	6	4
10^3	210	150	105	75	52	36
10^4	1700	1300	900	600	420	360
10^5	11000	8500	6300	4100	2800	2000

TABLE 2. DIFFUSION COEFFICIENT, σ_z, M

	A	B	C	D	E	F
10^2	14	11	7.6	4.8	3.6	2.2
10^3	500	120	70	32	24	14
10^4	-	-	420	140	90	46
10^5	-	-	2100	440	170	92

The meteorological categories can be characterized as follows [7][1].

1 ≡ A = extremely unstable conditions

2 ≡ B = moderately unstable conditions

3 ≡ C = slightly unstable conditions

4 ≡ D = neutral conditions (applicable to heavy overcast, night or day)

5 ≡ E = slightly stable conditions

6 ≡ F = moderately stable conditions.

The categories A-F relate to surface wind speed, insolation, and percent of overcast as shown in the following table [7].

Surface Wind Speed Meters/Sec	Daytime Insolation			Thin Overcast or ≥ 4/8 Cloudiness	≤ 3/8 Cloudiness
	Strong	Moderate	Slight		
< 2	A	A-B	B		
2	A-B	B	C	E	F
4	B	B-C	C	D	E
6	C	C-D	D	D	D
> 6	C	D	D	D	D

Some comments about the stability classes and corresponding σ_y, σ_z values are in order. There exists a "G" category of stability which will not be considered here. This category requires a negative thermal radiation balance. The G category may thus occur only at night. The F category is also primarily a night-time reading, though F may extend beyond sunrise on the order of one hour. There is hesitancy on the part of some authors to use F (and G) class stability since an averaging process outside of the direct time period of applicability would yield false averages. References 8 and 9 treat F (and G) as common cases.

1. For numerical convenience we shall relabel class A as 1 through class F as 6.

Since the period of worst meteorological conditions with respect to pollution propagation does not occur at the same general time as does peak traffic loads, care must be taken that realistic combinations are used. Even so, one of the following graphs will deal exclusively with F class stability in order to illustrate conditions which could exist under special circumstances.

The numerical values of the σ_y, σ_z parameters must also be used with care. These are intended for fairly short range calculations[2]. Specifically, many of the values of σ_y and σ_z given in Tables 1 and 2 are apparently the result of extrapolations rather than measured data.

For this reason, we shall restrict the numerical use of the equations to a distance of one kilometer for $x - x_o$.

Reference 10 contains valuable data concerning the calculation of the σ values. In this source, the values of these parameters are shown as a functional equality involving the wind equation angle, the vertical virtual distance, vertical diffusion, and the distance over which rectilinear vertical expansion occurs downwind from an ideal point source. This approach could be used if one were attempting to isolate the exact set of meteorological parameters which correspond to worst case estimates. Even so, certain assumptions must be made with respect to the input variables to the equation unless massive quantities of statistics on meteorological patterns are available. For this reason it is convenient to use the values given in Tables 1 and 2 for values of $x - x_o \leqslant 10^3$ meters.

There are other important parameters in the equations which have been developed besides the σ_y, σ_z values. The parameter H, the height of stabilization of the center of the pollutant cloud, drastically affects the numerical results, H, or its equivalent, is almost inevitably included in all but the most elementary diffusion models. Specifically, rocket exhaust plumes during static firing have flow rates and heat contents which are extremely large. This gives rise to very high stabilization heights. Furthermore, stack gas emissions from power generation and industrial sources sometimes are designed to yield a maximum value of H within economic and materials constraints. In the case of automotive pollution, H is very much smaller than are the values for either rocket plumes or industrial stacks.

An equation suitable for estimating H for automotive exhaust is given in Reference 10. Assuming the radius of the exhaust pipe to be effectively zero we have, from [10],

---

2. Stephens, J. Brisco: Personal Communications.

$$H = \left(\frac{8G}{\xi^3 \eta}\right)^{1/4} ,$$

where:

G is the buoyancy parameter, $(3\ g\eta/\mu\pi\rho c_p\tau)$,

ζ is the effective heat released,

ρ is the density of anbient air,

c_p is the ratio of specific heats of air at constant pressure,

τ the temperature,

ξ the entrainment coefficient,

η is defined at $\frac{g}{\tau}\frac{\partial\theta}{\partial z}$, and

g is the acceleration of gravity.

The quantity $\frac{\partial\theta}{\partial z}$ is defined by the subsidiary relationship

$$\frac{\partial\theta}{\partial z} = \frac{\partial\tau}{\partial z} + \frac{g}{c_p}$$

Apparently fewer estimates have been given for the flow rate and exhaust temperature of automobiles than have been given for certain other characteristics of these machines. Two sources which list the flow rate and temperatures of automotive engines are References 10 and 11. Reference 10 gives the following table, which is the more complete of the two sources.

TABLE 3. ENGINE EXHAUST DATA

		Driving Mode			
		Idle	Acceleration	Cruise	Deceleration
Exhaust Flow	C.F.M.	5-25	40-200	25-60	5-25
	m^3/min	0.14-5.66	1.13-5.66	0.71-1.70	0.14-0.71
Exhaust Gas Temp.*	°F	150-300	450-700	400-600	200-400
	°C	65.6-149	232-371	204-316	93-204

* At the entrance to the muffler.

Additionally, a temperature profile for the atmospheric layer in the 1.2 to 7.1 meter region is given in Reference 4.

A very careful calculation would involve estimates of the percentage of time in each driving mode. But the calculations with limit cases indicate a rather high insensitivity to various inputs since H involves a fourth root. Specifically, although the temperatures listed above are almost surely much too high for the actual temperature of the gas emerging at the tailpipe, there seems no need for further precision. The estimates range from approximately one-half meter to about three and one-half meters, with two meters being a good number. This will be used in subsequent calculations. (The numerical range assumed for ξ for an H value of two meters is 0.11 to 0.16).

In order to illustrate the primitive use of the diffusion relationship, a simple case will be presented, using a linear road which is orthogonal to the direction of the wind. Furthermore, a constant flow of 1000 vehicles per hour will be used in order that specific traffic flow patterns do not muddle the overall picture. The length of the road will be specified at 2 kilometers. The mixing layer depth, l, will be treated parametrically, and the road width given at 10 meters.

Initial parameter variations will involve the distance from the road and the meteorological categories. To obtain results of general application, χ/Q will be reported rather than χ and Q per se. The y and z coordinates used below are arbitrarily set as (0,2) respectively.

NUMERICAL RESULTS

The most obvious data which can be generated from the program concerns the reduction of pollution as one moves away from the road. This is plotted in Figure 7. This data was generated under the assumption of class 6 stability – which is probably overly severe, but acts as a bounding case. Notice that for constant traffic density, the parameter $\bar{u}$ enters hyperbolically, so that only one value of $\bar{u}$ needs to be actually programmed.

For a given wind speed, it is also of interest to illustrate the variation of χ/Q with distance for varying stability classes. This is shown in Figure 8. This Figure also assumes a mixing layer depth of 1000 meters. The figure shows the importance of stability class variation with respect to pollution concentration. For a very unstable atmosphere (stability class 1 or A), pollutants are quickly dispersed due to upward ventilation. As the atmosphere becomes progressively more stable, less and less vertical mixing occurs, resulting in higher concentrations near the ground.

$$\left(\frac{3\xi T^2}{2\bar{u}^2}\right)^{\frac{1}{3}}$$

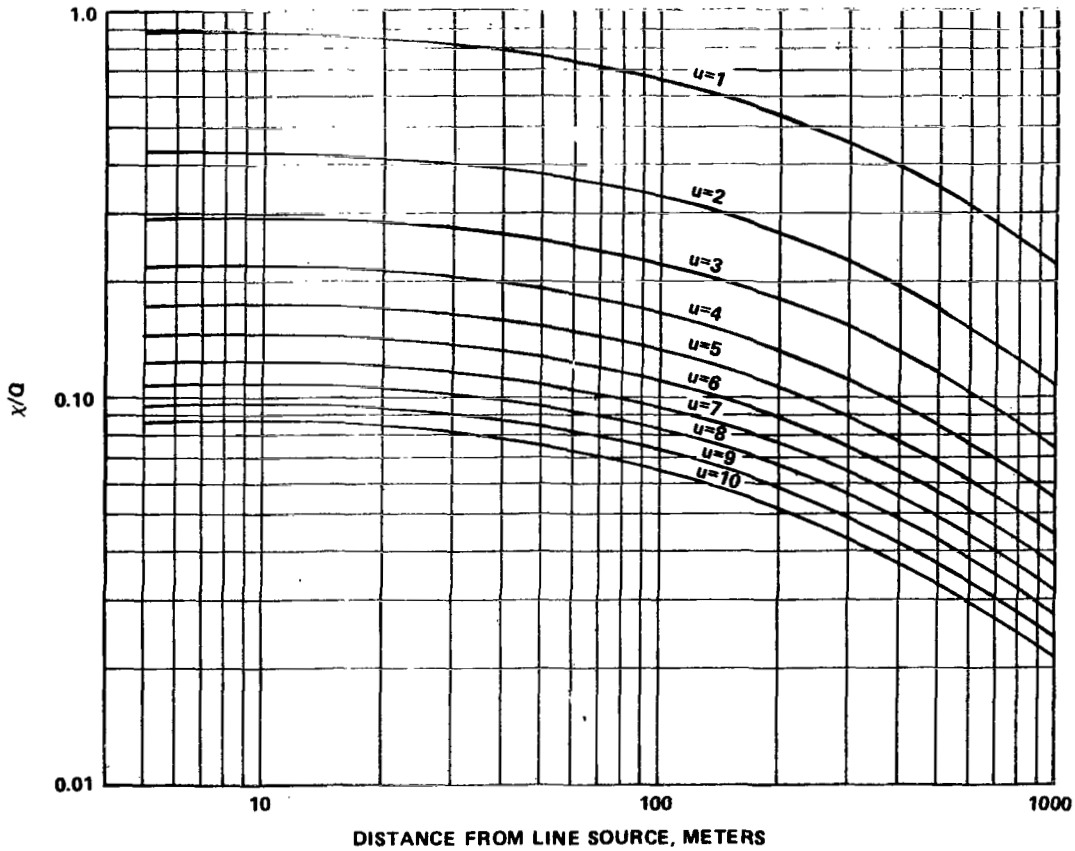

Figure 7. Variation of χ/Q versus distance from line source, with wind speed as a parameter (stability class 6(F)-mixing layer depth 1000m).

Rather than dealing directly with varying χ/Q, it is also of interest to fix the value of χ/Q via variation of wind speed. That is, for a given distance there is some wind speed which corresponds to a value of $\chi/Q = e^{-2}$. Since distance and wind speed, at which $\chi/Q = e^{-2}$, depends upon the stability class and the mixing layer depth, these additional variables must also be reckoned with. In Figure 9, the mixing layer depth is 1000 meters and the stability categories are shown parametrically. Thus, for a given stability class and a mixing layer depth of 1000 meters, we can find the distance at which χ/Q is equal to e^{-2} for a given wind speed.

In Figure 10 we have the same plot as Figure 9, excepting the fact that the mixing layer depth is only 100 meters. It is interesting to note that even this drastic decreases modifies the results only for stability class 1 and then only for distances beyond several hundred meters. The effect would eventually modify all stability classes at further distances, of course.

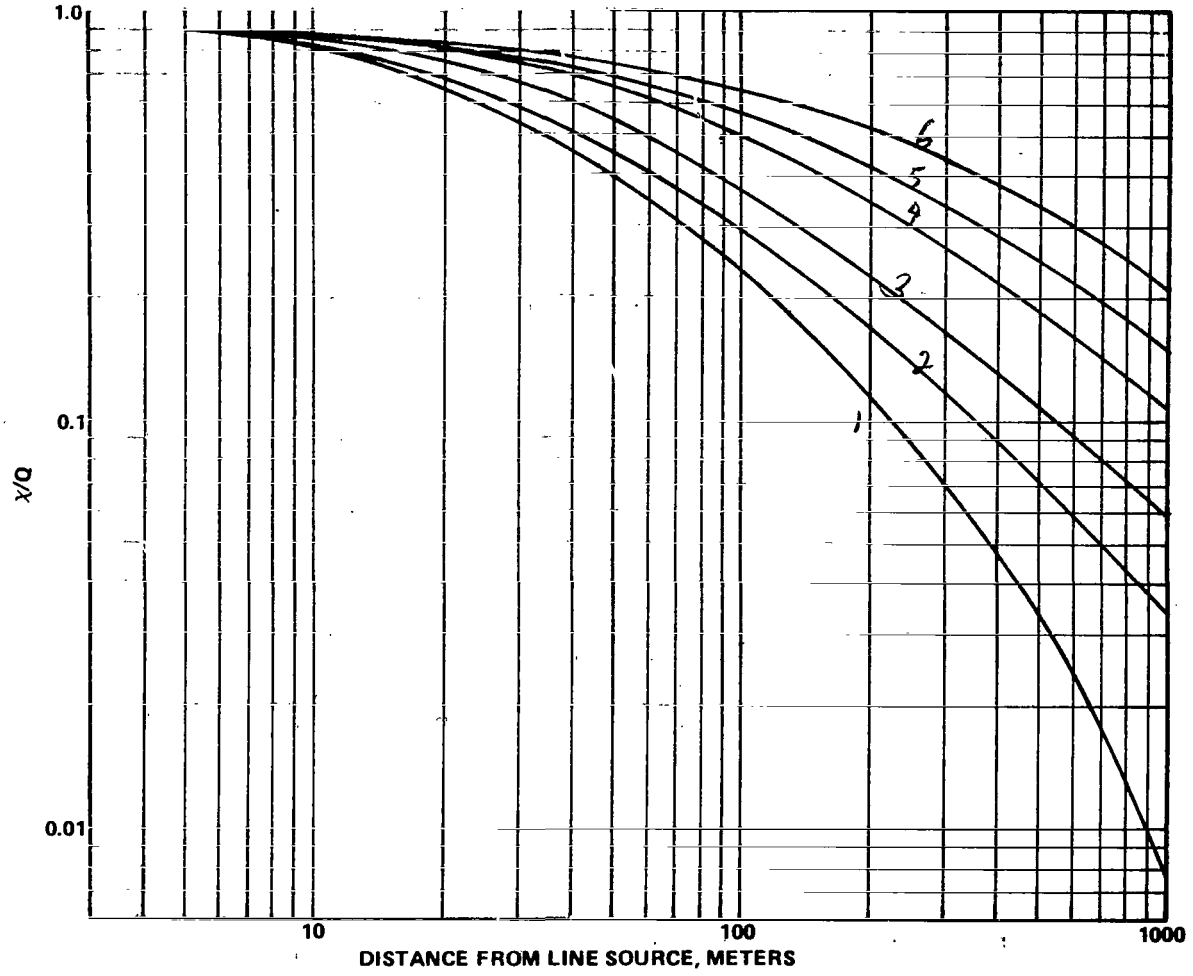

Figure 8. Variation of χ/Q versus distance from line source, with stability class as a parameter (wind speed 1 m/sec – mixing layer depth 1000 meters).

Figure 11 indicates the result of a further reduction in mixing layer depth. The case illustrated has a mixing layer depth of only 10 meters -- a low but physically realistic value. The result is obvious for all stability classes - namely, the pollutants are trapped near the ground and concentration becomes almost independent of distance.

The next three graphs, Figures 12, 13, and 14 are cross plots of the data shown in the preceeding three graphs. In each case, the wind speed necessary to achieve the value of $\chi/Q^* = e^{-2}$ at the parametric distances is plotted against mixing layer depth.

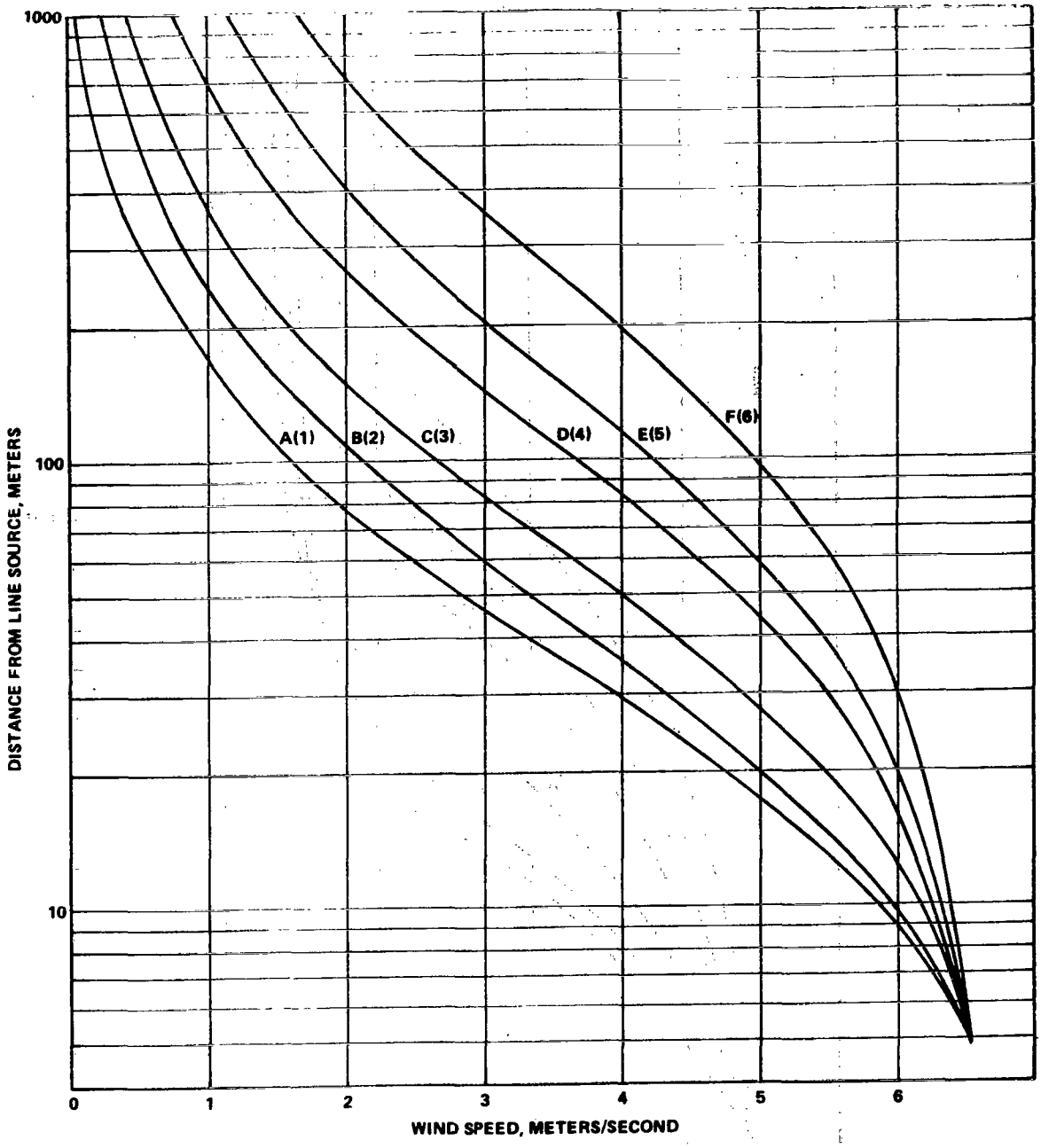

Figure 9. Distance from line source at which $\chi/Q = 1/e^2$ versus wind speed, with stability class as a parameter (mixing layer depth 1000 meters).

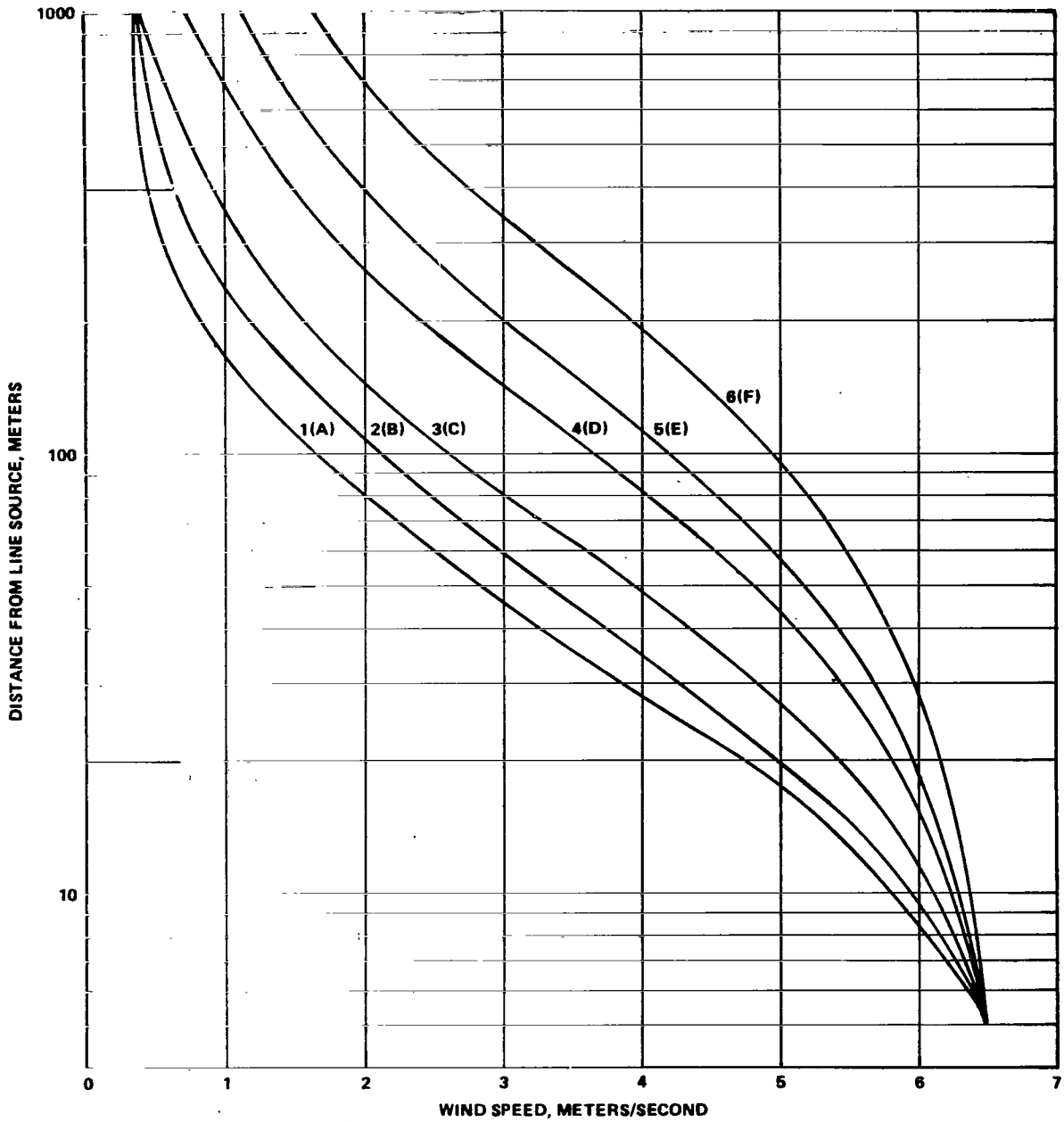

Figure 10. Distance from line source at which $\chi/Q = e^{-2}$ versus wind speed, with stability class as a parameter (mixing layer depth 100 meters).

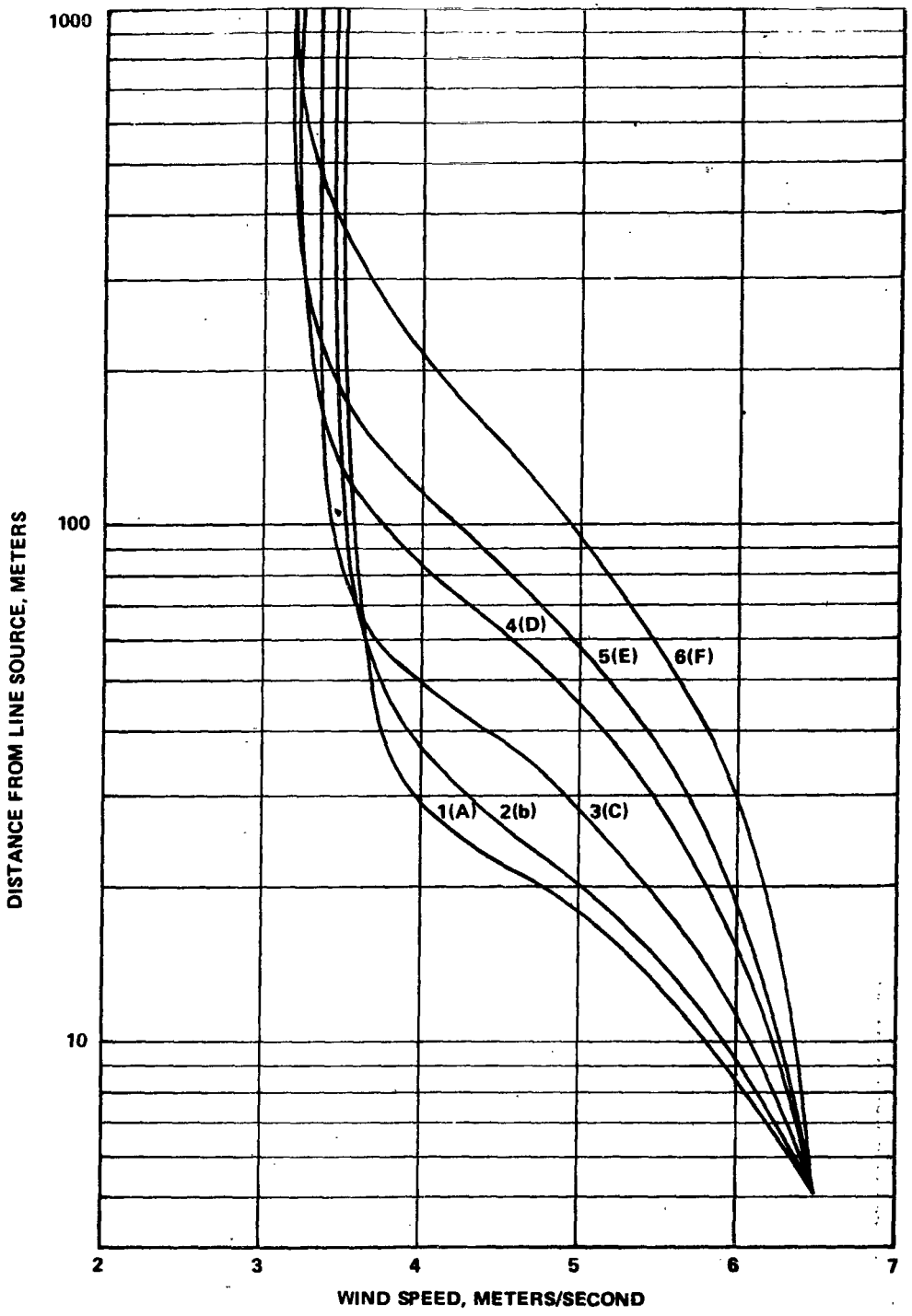

Figure 11. Distance from line source at which $\chi/Q = e^{-2}$ versus wind speed, with stability class as a parameter (mixing layer depth 10 meters).

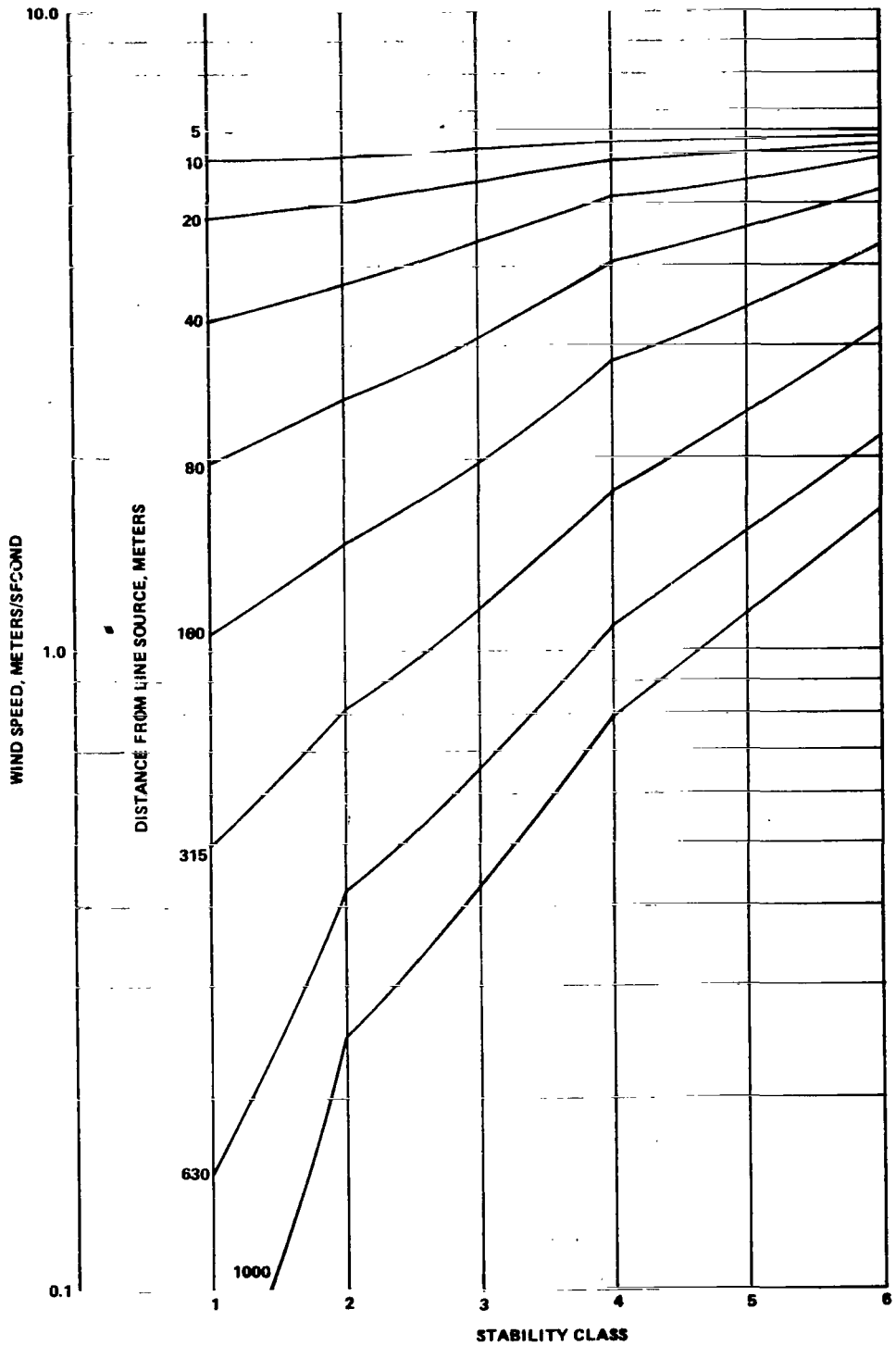

Figure 12. Wind speed required to achieve $\chi/Q = e^{-2}$ at the parametric distance versus stability class (mixing layer depth 1000 meters).

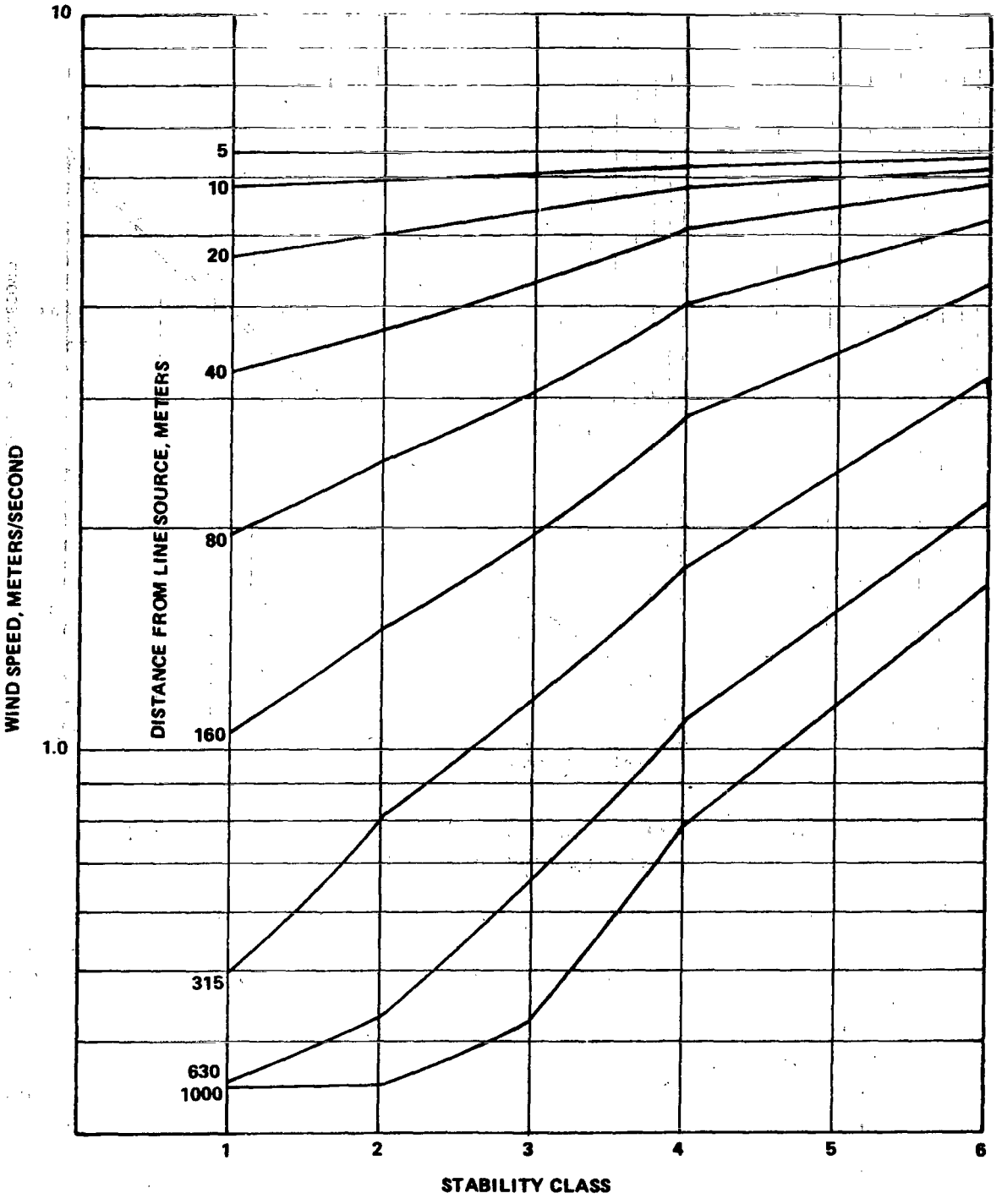

Figure 13. Wind speed required to achieve $\chi/Q = e^{-2}$ at the parametric distance versus stability class (mixing layer depth 100 meters).

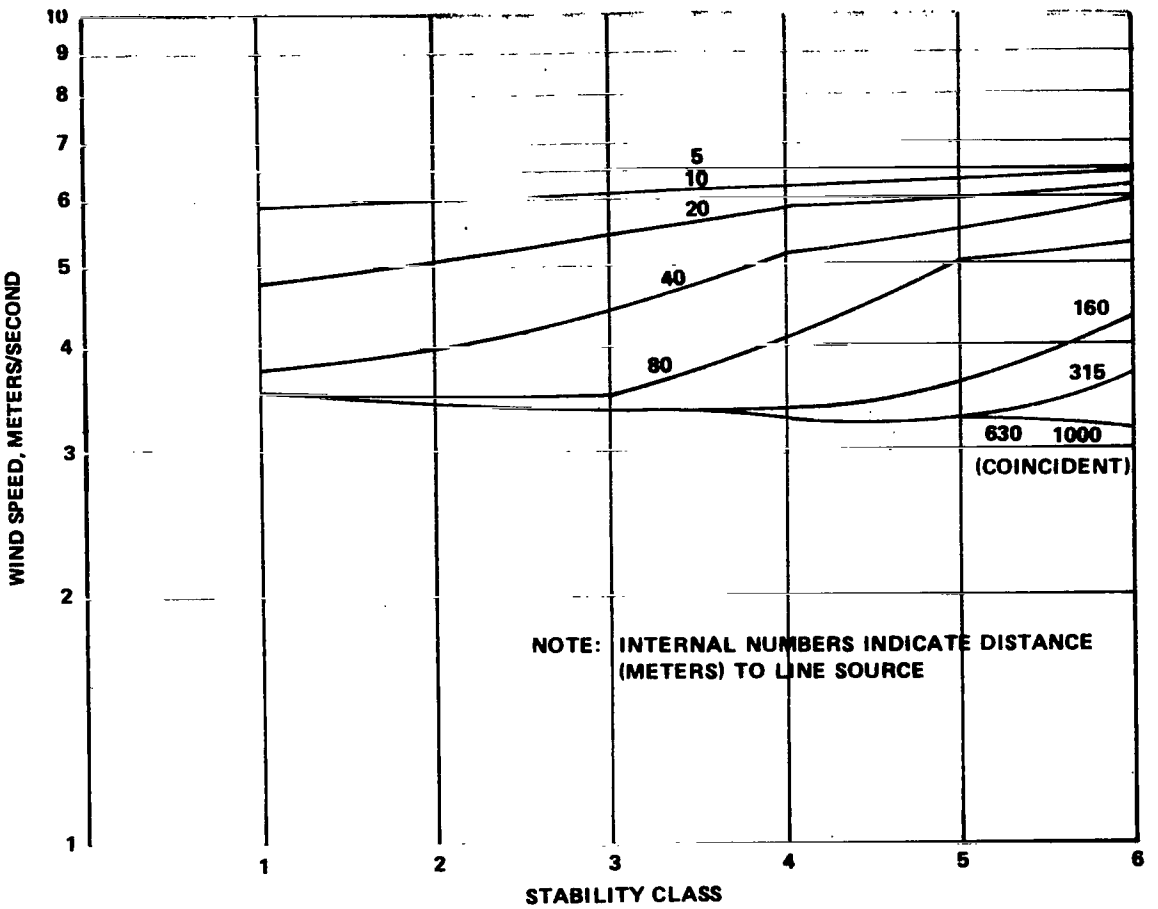

Figure 14. Wind speed necessary to achieve $\chi/Q = e^{-2}$ at the parametric distance versus stability class (mixing layer depth 10 meters).

The three figures differ in having mixing depths of 1000, 100, and 10 meters, respectively. The representation of the data in this form is particularly useful if a statistical study of probable weather pattern is to be used to predict potential pollution levels.

In the above mentioned charts, the mixing layer depths were never taken above 1000 meters. The reason for this limitation is that 1000 meters is an asymptotic value insofar as diffusion over the x coordinate range of 1000 meters is concerned. In other words, values of mixing depth above 1000 meters give no significant variation from a mixing layer depth of 1000 meters.

This point is further illustrated in Figure 15. The wind speed necessary to achieve a χ/Q of e^{-2} at 1000 meters versus mixing layer depth is illustrated in this case, with stability class as a parameter. From this graph it is apparent that lower mixing ceilings

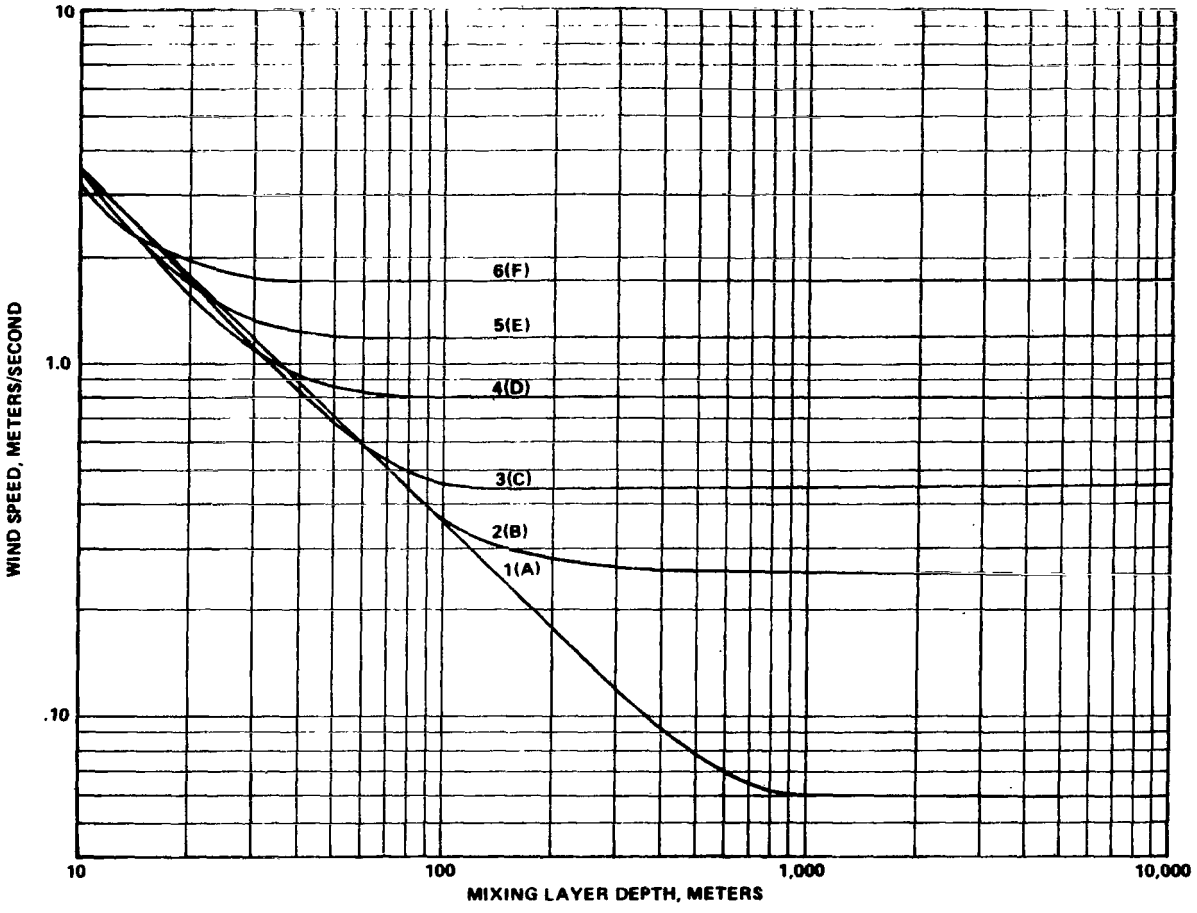

Figure 15. Wind speed necessary to achieve $\chi/Q = e^{-2}$ at 1000 meters versus mixing layer.

most strongly affects the most unstable atmospheric conditions. This may be intuitively understood as follows. The basic equations for describing the mixing lid reflections is the method of infinite imaging, equation (16) and the modifications that follow from it. Under extremely unstable conditions (say, 1 or A conditions) then a cell of pollutant would tend to rise very rapidly, and thus be "reflected" at an earlier point than would a cell of pollution under more stable conditions. Thus, Figure 15 corresponds to physical intuition.

CONCLUSIONS

It has been shown that the standard diffusion equation may be separated to yield solutions which interface with known geometric and meteorological constraints. Specific weather conditions were assumed to illustrate the application of the theory.

It was seen that under the assumption of constant traffic density on a linear road, the worst weather conditions involve a rather stable atmosphere and low wind speed. The depth of the mixing layer seems relatively unimportant of the first kilometer from the line source, unless very low mixing depths are encountered.

Under the very special conditions of small mixing depths, the most stable atmosphere may, at adequate distance, actually produce a lower concentration of pollutants than an unstable atmosphere.

APPENDIX A

BASIC COMPUTER PROGRAM

```
C     SUBROUTINE LGINT(LAGRANGIAN INTERPOLATION)  JRA 12/12/72
C     CCCCCCCCCCCCCCCCCCCCCCCCCCCCCCCCCCCCCCCCCCCCCCCCCCCCCCCCCCCCCCCCCCC
C     C                                                                   C
C     C  SUBROUTINE LGINT PERFORMS LAGRANGIAN INTERPOLATION USING A       C
C     C  SPECIFIED NUMBER OF THE DATA POINTS IN THE GIVEN TABLE.          C
C     C                                                                   C
C     C                                                                   C
C     C  SUBROUTINE'S ARGUMENTS ARE...                                    C
C     C                                                                   C
C     C    XTABL--ARRAY OF INDEPENDENT VALUES OF DATA TABLE.              C
C     C                                                                   C
C     C    YTABL--ARRAY OF DEPENDENT VALUES OF DATA TABLE, VALUES         C
C     C           ARE IN DIRECT CORRESPONDENCE WITH XTABL VALUES.         C
C     C                                                                   C
C     C    NTABL--LENGTH OF XTABL AND YTABL ARRAYS.                       C
C     C                                                                   C
C     C    X     --INDEPENDENT VALUE FOR WHICH A CORRESPONDING            C
C     C            DEPENDENT VALUE IS TO BE INTERPOLATED.                 C
C     C                                                                   C
C     C    Y     --THE INTERPOLATED DEPENDENT VALUE.                      C
C     C                                                                   C
C     C    NPTS --NUMBER OF POINTS FROM THE TABLE TO BE USED IN THE       C
C     C           INTERPOLATION.                                          C
C     C                                                                   C
C     C    IERR --ERROR INDICATOR  IERR=1  INTERPOLATION PERFORMED        C
C     C                                    CORRECTLY                      C
C     C                            IERR=2  INTERPOLATION INHIBITED        C
C     C                                    BECAUSE X OUTSIDE TABLE,       C
C     C                                    NPTS LESS THAN 1, OR NPTS      C
C     C                                    GREATER THAN NTABL.            C
C     C                                                                   C
C     C  SUBROUTINE'S IMPORTANT VARIABLES...                              C
C     C                                                                   C
C     C    NONE                                                           C
C     C                                                                   C
C     C  LIMITATIONS...                                                   C
C     C                                                                   C
C     C    VALUES OF XTABL ARRAY MUST BE STRICTLY INCREASING.             C
C     C                                                                   C
C     C    X GREATER THAN OR EQUAL TO XTABL(1) AND LESS THAN OR EQUAL     C
C     C    TO XTABL(NTABL).                                               C
C     C                                                                   C
C     C    NPTS GREATER THAN OR EQUAL TO 1 AND LESS THAN OR EQUAL         C
C     C    TO NTABL.                                                      C
C     C                                                                   C
C     C  NOTES...                                                         C
C     C                                                                   C
C     C    LGINT IS LIMITED TO INTERPOLATION, IT WILL NOT EXTRAPOLATE.    C
C     C                                                                   C
C     C    ONE POINT INTERPOLATION RETURNS THE YTABL VALUE WITH           C
C     C    THE CORRESPONDING XTABL VALUE THAT IS CLOSEST TO X.            C
C     C                                                                   C
C     C    TWO POINT INTERPOLATION IS EQUIVALENT TO LINEAR                C
C     C    INTERPOLATION USING THE TWO POINTS.                            C
C     C                                                                   C
C     C    THE TABLE VALUES USED IN THE INTERPOLATION ARE CENTERED        C
C     C    AROUND THE POINT OF INTERPOLATION WHEN POSSIBLE.  HOWEVER,     C
C     C    WHEN THE INTERPOLATION POINT IS CLOSE TO EITHER END OF         C
C     C    THE TABLE,  THE TABLE VALUES USED ARE THAT END OF              C
C     C    THE TABLE.                                                     C
C     C                                                                   C
```

```
C      C  PROGRAMMER--JAMES R. ALEXANDER                                    C
C      CCCCCCCCCCCCCCCCCCCCCCCCCCCCCCCCCCCCCCCCCCCCCCCCCCCCCCCCCCCCCCCCCCCC
       SUBROUTINE LGINT(XTABL,YTABL,NTABL,X,Y,NPTS,IERR)
       DIMENSION XTABL(1),YTABL(1)
       IERR=1
C
C      ERROR CHECKS
C
       IF(NPTS)20,20,10
   10  IF(NPTS-NTABL)30,30,20
   20  IERR=2
       RETURN
C
C      INTERPOLATION INHIBITED--VALUE OF NPTS OUT OF PERMISSIBLE RANGE
C      LOCATING PORTION OF TABLE TO BE USED IN INTERPOLATION
C
   30  I=1
       I2=2*(NTABL-1)
       NC=NTABL
       I1=1
   40  IF(X-XTABL(I))60,50,70
   50  Y=YTABL(I)
       RETURN
   60  I2=I
       NC=I
       GO TO 80
   70  I1=I
   80  I=(I2-I1+1)/2+I1
       I2=NC
       IF(I2-I1-1)90,100,40
   90  IERR=2
       RETURN
C
C  INTERPOLATION INHIBITED--VALUE OF X OUTSIDE RANGE OF XTABL VALUES
C
  100  NC=I2
       IF(XTABL(I2)+XTABL(I1)-2.0*X)120,120,110
  110  NC=I1
  120  I1=I1-NPTS/2+1-(NPTS-NPTS/2*2)*(I1/NC)
       I2=I1+NPTS-1
       IF(I1)130,130,140
  130  I1=1
       I2=NPTS
       GO TO 160
  140  IF(I2-NTABL)160,160,150
  150  I1=NTABL-NPTS+1
       I2=NTABL
C
C  PERFORM INTERPOLATION
C
  160  Y=0.0
       DO 190 I=I1,I2
       YY=1.0
       DO 180 J=I1,I2
       IF(I-J)170,180,170
  170  YY=YY*(X-XTABL(J))/(XTABL(I)-XTABL(J))
  180  CONTINUE
  190  Y=Y+YY*YTABL(I)
       RETURN
       END
```

```
      FUNCTION SIGY(X,VIS)
C
C  FUNCTION SIGY DETERMINES THE HORIZONTAL DISPERSION COEFFICIENT
C  TABLE OF VALUES TAKEN FROM,  WORKBOOK OF ATMOSPHERIC DISPERSION
C                               ESTIMATES, D. BRUCE TURNER, PUBLIC
C                               HEALTH SERVICE, 1970--AVAILABLE AS
C                               PB-191482 OR N71-31626.
C                               SEE FIGURE 3-2.
C  X     --DISTANCE DOWNWIND
C  VIS   --STABILITY CLASS 1=A,....,6=F.  A NON INTEGER VALUE RESULTS
C         IN LINEAR INTERPOLATION IN THE LOGX-LOGSIGY SPACE BETWEEN
C         THE TWO NEAREST CLASSES
C
      DIMENSION FY(16,6)
      DIMENSION F1(16),F2(16),F3(16),F4(16),F5(16),F6(16)
      EQUIVALENCE (FY(1),F1(1)),(FY(17),F2(1)),(FY(33),F3(1))
      EQUIVALENCE (FY(49),F4(1)),(FY(65),F5(1)),(FY(81),F6(1))
      DATA F1/27.5,41.5,62.0,95.0,140.0,215.0,325.0,470.0,715.0,
     11040.0,1590.0,2300.0,3350.0,4900.0,7250.0,11000.0/
      DATA F2/19.5,29.0,44.5,68.0,100.0,158.0,238.0,360.0,550.0,800.0,
     11190.0,1800.0,2600.0,3850.0,5580.0,8200.0/
      DATA F3/12.5,19.2,34.0,45.5,68.0,105.0,162.0,242.0,370.0,
     1550.0,840.0,1280.0,1880.0,2800.0,4150.0,6100.0/
      DATA F4/8.1,12.3,19.0,28.5,44.0,68.0,108.0,160.0,247.0,370.0,
     1560.0,840.0,1220.0,1820.0,2700.0,4100.0/
      DATA F5/6.1,9.3,14.2,21.8,33.0,51.0,78.0,118.0,180.0,275.0,
     1410.0,630.0,830.0,1380.0,2050.0,3050.0/
      DATA F6/4.1,6.2,9.3,14.8,22.0,34.0,53.0,79.0,122.0,180.0,
     1275.0,420.0,620.0,940.0,1380.0,2050.0/
      A(X)=0.43429*ALOG(X)
      N=1
      IF(X-1.0)10,20,20
   10 SIGY=0.0
      RETURN
   20 IF(X-100000.0)30,30,10
   30 I1=VIS+0.1
      I2=I1+1-I1/6
      IF(I1)10,10,40
   40 IF(I1-6)50,50,10
   50 IF(X-160.0)70,70,60
   60 N=1.0001+(A(X)-2.0)*5.0
   70 Y1=A(FY(N,I1))+A(FY(N,I2)/FY(N,I1))*(VIS-FLOAT(I1))
      Y2=A(FY(N+1,I1))+A(FY(N+1,I2)/FY(N+1,I1))*(VIS-FLOAT(I1))
      SIGY=10.0**(Y1+(Y2-Y1)/0.2*(A(X)-2.0-(N-1)*0.2))
      RETURN
      END
```

```
      FUNCTION SIGZ(X,VIS)
C
C  FUNCTION SIGZ DETERMINES THE VERTICAL DISPERSION COEFFICIENT
C  TABLE OF VALUES TAKEN FROM,  WORKBOOK OF ATMOSPHERIC DISPERSION
C                               ESTIMATES, D. BRUCE TURNER, PUBLIC
C                               HEALTH SERVICE, 1970--AVAILABLE AS
C                               PB-191482 OR N71-31626.
C                               SEE FIGURE 3-3.
C  X     --DISTANCE DOWNWIND
C  VIS   --STABILITY CLASS 1=A,...,6=F.  A NON INTEGER VALUE RESULTS
C          IN LINEAR INTERPOLATION IN THE LOGX-LOGSIGZ SPACE BETWEEN
C          THE TWO NEAREST CLASSES
C
      DIMENSION FZ(16,6)
      DIMENSION F1(16),F2(16),F3(16),F4(16),F5(16),F6(16)
      EQUIVALENCE (FZ(1),F1(1)),(FZ(17),F2(1)),(FZ(33),F3(1))
      EQUIVALENCE (FZ(49),F4(1)),(FZ(65),F5(1)),(FZ(81),F6(1))
      DATA F1/14.0,23.0,37.0,72.0,170.0,465.0,1220.0,3100.0,8600.0,
     121500.0,60000.0,140000.0,315000.0,740000.0,1650000.0,4200000.0
      DATA F2/11.0,16.5,25.5,41.0,65.0,110.0,185.0,300.0,500.0,
     1820.0,1380.0,2250.0,3750.0,6200.0,10200.0,17000.0/
      DATA F3/7.4,11.5,17.0,26.3,39.5,61.0,95.0,142.0,220.0,330.0,
     1510.0,780.0,1150.0,1800.0,2650.0,3900.0/
      DATA F4/4.7,7.0,10.3,15.8,22.2,32.0,43.8,58.0,77.0,101.0,
     1138.0,180.0,230.0,295.0,365.0,460.0/
      DATA F5/3.6,5.3,7.7,11.0,15.3,21.2,29.0,38.5,50.0,62.0,79.0,
     1100.0,120.0,143.0,163.0,183.0/
      DATA F6/2.3,3.4,4.9,7.1,10.2,14.0,19.0,24.0,31.0,37.5,46.5,
     156.0,64.0,73.0,84.0,94.0/
      A(X)=0.43429*ALOG(X)
      N=1
      IF(X-1.0)10,20,20
   10 SIGZ=0.0
      RETURN
   20 IF(X-100000.0)30,30,10
   30 I1=VIS+0.1
      I2=I1+1-I1/6
      IF(I1)10,10,40
   40 IF(I1-6)50,50,10
   50 IF(X-160.0)70,70,60
   60 N=1.0001+(A(X)-2.0)*5.0
   70 Y1=A(FZ(N,I1))+A(FZ(N,I2)/FZ(N,I1))*(VIS-FLOAT(I1))
      Y2=A(FZ(N+1,I1))+A(FZ(N+1,I2)/FZ(N+1,I1))*(VIS-FLOAT(I1))
      SIGZ=10.0**(Y1+(Y2-Y1)/0.2*(A(X)-2.0-(N-1)*0.2))
      RETURN
      END
```

```
      FUNCTION CHIF3(FX,Z,HIL,H)
C
C  FUNCTION CHIF3 EVALUATES THE Z-X DEPENDENCY OF CHI
C  FX    --THE VERTICAL DISPERSION COEFFICIENT AT X
C  Z     --Z COORDINATE
C  HIL   --HEIGHT OF INVERSION LAYER
C  H     --SOURCE HEIGHT
C  SERIES IS SUMMED UNTIL NTH TERM CONTRIBUTES LESS THAN 0.01 PERCENT
C  TO THE N TERMS OF THE SERIS.
C
      C=0.5/(FX*FX)
      R=Z+H
      S=Z-H
      F=EXP(-C*R*R)+EXP(-C*S*S)
      N=1
   10 Q=FLOAT(2*N)*HIL
      FN=EXP(-C*(S-Q)*(S-Q))+EXP(-C*(R+Q)*(R+Q))+EXP(-C*(R-Q)*(R-Q))
     1+EXP(-C*(S+Q)*(S+Q))
      F=F+FN
      N=N+1
      IF(FN/F-0.0001)20,10,10
   20 CHIF3=F
      RETURN
      END



      FUNCTION CHIF4(HX,Y,Y0)
C
C  FUNCTION CHIF4 EVALUATES THE Y-X DEPENDENCY OF CHI
C  HX    --THE HORIZONTAL DISPERSION COEFFICIENT AT X
C  Y     --Y COORDINATE
C  Y0    --ROAD SEGEMENT HALF LENGTH
C
C
C  REAL ERROR FUNCTION APPROXIMATION
C    ERF(X) = ERFA(X) + E,  X GREATER THAN OR EQUAL TO ZERO
C    ABS(E) LESS THAN OR EQUAL TO 1.5E-07
C  REFERENCE.  ABRAMOWITZ, M. AND STEGUN, I. A.  HANDBOOK OF
C              MATHEMATICAL FUNCTIONS, NATIONAL BUREAU OF STANDARDS,
C              APPLIED MATHEMATICS SERIES.55, JUNE 1964, PAGE 299,
C              EQUATION 7.1.26.
C
      S(X)=1.0/(1.0+0.3275911*X)
      ERFA(X)=1.0-(S(X)*(0.254829592+S(X)*(-0.284496736+S(X)*
     1         (1.421413741+S(X)*(-1.453152027+S(X)*1.061405429)))))*
     2         EXP(-X*X)
C
C
      C=HX*1.41421356
      Y1=Y0-Y
      Y2=Y0+Y
      CHIF4=SIGN(ERFA(ABS(Y1)/C),Y1)+SIGN(ERFA(ABS(Y2)/C),Y2)
      RETURN
      END
```

```
** PROGRAM CHITR(PREDICTION OF STRAIGHT ROAD AIR POLLUTION)  07/28/73
      DIMENSION TT(50),PHI(50)
      IRD=2
      IPR=3
C  SIGZM IS THE VERTICAL DISPERSION ASSUMED TO HAVE OCCURED
C  FROM VEHICLE INDUCED MIXING.
      SIGZM=2.4
C  READ TRAFFIC TIME DENSITY(TIME IN UNITS USED BELOW, VEHICLES/SEC)
C  DENSITY FUNCTION IS USED CYCLICALLY
      READ(IRD,1) N,(TT(I),PHI(I),I=1,N)
    1 FORMAT(I5/(2F8.2))
      TTT=TT(N)-TT(1)
C  READ EMMISSION/METER-VEH, ROAD HALF LENGTH,SOURCE HEIGHT, INVERSION
C  LAYER HEIGHT, ROAD HALF WIDTH, WIND VELOCITY, AND STABILITY CLASS
C  (1.0=A,...,6.0=F)
      READ(IRD,2) Q,YO,H,HIL,XM,U,VIS
    2 FORMAT(10F8.2)
C  CALCULATE X BIAS FOR INITIAL DISPERSION
      Y1=SIGZ(1.0,VIS)
      Y2=SIGZ(100.0,VIS)
      XB=10.0**(2.0*ALOG(SIGZM/Y1)/ALOG(Y2/Y1))
      SIGYO=SIGY(XM+XB,VIS)
      SIGZO=SIGZ(XM+XB,VIS)
      C1=1.0/CHIF3(SIGZO,0.0,HIL,H)
      C2=1.0/CHIF4(SIGYO,0.0,YO)
      C=Q/H/U*SIGZO*C1*C2
C  READ NUMBER OF PREDICTIONS
      READ(IRD,7) NPRED
    7 FORMAT(I5)
      DO 100 IPRED=1,NPRED
C  READ SPATIAL AND TEMPORAL COORDINATES OF PREDICTION POINT
      READ(IRD,2) X,Y,Z,T
      IF(X-XM)75,40,40
   40 IF(Z)75,50,50
   50 IF(Z-HIL)80,80,75
   75 WRITE(IPR,5)
    5 FORMAT(1H1/10X,26HINPUT COORDINATES IN ERROR)
      GO TO 100
   80 SIGYX=SIGY(X+XB,VIS)
      SIGZX=SIGZ(X+XB,VIS)
      F1=1.0/SIGZX
      TP=T-(X-XM)/U
      M=ABS(TP/TTT)
      IF(TP-TT(1))82,83,83
   82 TP=TP+TTT*(M+1)
   83 IF(TP-TT(N))85,85,84
   84 TP=TP-TTT*M
   85 CALL LGINT(TT,PHI,N,TP,F2,2,IERR)
      GO TO(95,90),IERR
   90 WRITE(IPR,6) TP
    6 FORMAT(1H1/10X,19HINTERPOLATION ERROR/10X,F8.2)
      GO TO 100
   95 F3=CHIF3(SIGZX,Z,HIL,H)
      F4=CHIF4(SIGYX,Y,YO)
      CHI=C*F1*F2*F3*F4
      WRITE(IPR,3) X,Y,Z,T,CHI
    3 FORMAT(1H1/10X,4HCHI(,F8.2,1H,,F8.2,1H,,F8.2,1H,,F8.2,4H) = ,
     1E12.5)
      WRITE(IPR,4) Q,YO,H,HIL,XM,U,VIS,XB,SIGYO,SIGZO,SIGYX,SIGZX,
     1C1,C2,C,F1,F2,F3,F4
    4 FORMAT(//10X,4HQ = ,E12.5/10X,5HYO = ,E12.5/
```

```
     110X,4HH = ,E12.5/10X,6HHIL = E12.5/10X,5HXM = ,E12.5/10X,4HU = ,
     2E12.5/10X,6HVIS = ,E12.5/10X,5HXB = ,E12.5/10X,8HSIGY0 = ,E12.5/
     310X,8HSIGZ0 = ,E12.5/10X,8HSIGYX = ,E12.5/10X,8HSIGZX = ,E12.5/
     410X,5HC1 = ,E12.5/10X,5HC2 = ,E12.5/10X,4HC = ,E12.5/10X,5HF1 = ,
     5E12.5/10X,5HF2 = ,E12.5/10X,5HF3 = ,E12.5/10X,5HF4 = ,E12.5)
 100 CONTINUE
     STOP
     END
```

APPENDIX B. EVALUATION OF CONTOUR INTERVAL

As previously mentioned, it is usually necessary to express pollution concentrations from a road when the wind vector is not orthogonal to the road. The specific integral for this task is shown on page 20.

In order to save computer time in the implementation of this case, it is often necessary to approximate the given integral analytically. To this end we proceed as follows.

If we agree to evaluate the integral for very large ℓ and at $z = H$ we have

$$\chi(x, y, H, t) = \frac{Q}{2}\,\sigma_z(x_0)\,\sigma_y(x_0)\int_{-y_0\tan\psi}^{y_0\tan\psi} \frac{e^{-\frac{(y - x^*\tan\psi)^2}{2\sigma_y^2(x - x^*)}} \sum_{p=1}^{M} b_p \sin P_p\left(t - \frac{x - x^* - x_0}{u}\right)^2}{\sigma_y(x - x^*)\,\sigma_z(x - x^*)}\,dx^* \qquad \text{(B-1)}$$

We now assume that

$$N(t) \simeq N\left(t - \frac{x - x^* - x_0}{\bar{u}}\right) ,$$

which will be valid for short segments. Then (B-1) becomes

$$\chi(x, y, H, t) = \frac{Q}{2}\,\sigma_z(x_0)\,\sigma_y(x_0)\,N(t)\int_{-y_0\tan\psi}^{y_0\tan\psi} \frac{e^{-\frac{(y - x^*\tan\psi)^2}{2\sigma_y^2(x - x^*)}}}{\sigma_y(x - x^*)\,\sigma_z(x - x^*)}\,dx^* .$$

For convenience we now write,

$$I = \int \frac{e^{-\frac{(y - x^*\tan\psi)^2}{2\sigma_y^2(x - x^*)}}}{\sigma_y(x - x^*)\,\sigma_z(x - x^*)}\,dx^* . \qquad \text{(B-2)}$$

Then,

$$y - x^* \tan\psi = y - x \tan\psi + x \tan\psi - x^* \tan\psi = (y - x \tan\psi) + (x - x^*) \tan\psi$$

Abbreviating,

$$(x - x^*) = r \qquad \text{(B-3)}$$

$$y - x \tan\psi = \eta \quad , \qquad \text{(B-4)}$$

we have

$$I = - \int \frac{e^{-\frac{(\eta + r \tan\psi)^2}{2\sigma_y^2 (r)}}}{\sigma_y (r)\, \sigma_z (r)}\, dr \quad .$$

We now approximate the reciprocal σ_y in the exponential as

$$\left[\sigma_y (r)\right]^{-1} = (\delta + \epsilon r) \quad , \qquad \text{(B-5)}$$

and operate on the resulting exponent as follows:

$$(\eta + r \tan\psi)^2 (\delta + \epsilon r)^2 = \left[\delta \eta + r (\delta \tan\psi + \epsilon \eta) + (\epsilon \tan\psi) r^2\right] \quad .$$

Substitute

$$s = r - \frac{(\delta \tan\psi + \epsilon \eta)}{2 \epsilon \tan\psi} \quad (\psi \neq 0) \quad , \qquad \text{(B-6)}$$

so that

$$(\eta + r \tan\psi)^2 (\delta + \epsilon r)^2 = (\epsilon \tan\psi) s^2 - \frac{(\delta \tan\psi - \epsilon \eta)^2}{4 \epsilon \tan\psi} \quad .$$

Then

$$I = e^{\frac{(\delta \tan \psi - \epsilon \eta)^2}{4 \epsilon \tan \psi}} \int \frac{e^{-(\epsilon \tan \psi) s^2}}{\sigma_y (s+\mu)\, \sigma_z (s+\mu)}\, ds \quad ,$$

with

$$\mu = \frac{(\delta \tan \psi - \epsilon \eta)}{4 \epsilon \tan \psi} \qquad \text{(B-7)}$$

Expand the σ_y and σ_z values that occur in the demoninator as

$$\frac{1}{\sigma_y (s+\mu)} = \sum_{i=0}^{3} \nu_i^* (s+\mu)^i \qquad \text{(B-8)}$$

$$\frac{1}{\sigma_z (s+\mu)} = \sum_{i=0}^{3} \nu_i^{**} (s+\mu)^i \qquad \text{(B-9)}$$

so that

$$\frac{1}{\sigma_y (s+\mu)\, \sigma_z (s+\mu)} = \sum_{i=0}^{6} \nu_i (s+\mu)^i \quad ,$$

where the ν_i's are defined as obvious combinations of ν_i^* and ν_i^{**} . Then

$$I = e^{\frac{(\delta \tan \psi - \epsilon \eta)^2}{4 \epsilon \tan \psi}} \sum_{i=0}^{6} \nu_i \int e^{-(\epsilon \tan \psi) s^2} (s+\mu)^i \, ds \quad .$$

Finally, setting

$$\sqrt{\epsilon \tan \psi}\, s = \omega \quad . \qquad \text{(B-10)}$$

so that

$$I = -e^{\frac{(\delta \tan\psi - \epsilon\eta)^2}{4\epsilon\tan\psi}} \sum_{i=0}^{6} \frac{\nu_i}{(\epsilon\tan\psi)^{\frac{i+1}{2}}} \int e^{-\omega^2} (\omega + \mu\sqrt{\epsilon\tan\psi})^i \, d\omega \quad . \tag{B-11}$$

The integral may now be evaluated from expressions contained in standard references such as Reference 12. From that scurce,

$$\int e^{-x^2} \, dx = \frac{\sqrt{\pi}}{2} \operatorname{erf} x \quad ,$$

$$\int x e^{-x^2} dx = -\frac{1}{2} e^{-x^2} \quad , \text{ and}$$

$$\int x^n e^{-x^2} \, dx = -\frac{1}{2} x^{n-1} e^{-x^2} + \frac{n-1}{2} \int x^{n-2} e^{-x^2} \, dx \quad .$$

The coefficients which occur in the expansion of the binominal are denoted as

$$D_0 = (\epsilon\tan\psi)^{-1/2} (\nu_0 + \nu_1\mu + \nu_2\mu^2 + \nu_3\mu^3 + \nu_4\mu^4 + \nu_5\mu^5 + \nu_6\mu^6) \quad ,$$

$$D_1 = (\epsilon\tan\psi)^{-1} (\nu_1 + 2\nu_2\mu + 3\nu_3\mu^2 + 4\nu_4\mu^3 + 5\nu_5\mu^4 + 6\nu_6\mu^5) \quad ,$$

$$D_2 = (\epsilon\tan\psi)^{-3/2} (\nu_2 + 3\nu_3\mu + 6\nu_4\mu^2 + 10\nu_5\mu^3 + 15\nu_6\mu^4) \quad ,$$

$$D_3 = (\epsilon\tan\psi)^{-2} (\nu_3 + 4\nu_4\mu + 10\nu_5\mu^2 + 20\nu_6\mu^3) \quad ,$$

$$D_4 = (\epsilon\tan\psi)^{-5/2} (\nu_4 + 5\nu_5\mu + 15\mu_6\mu^2) \quad ,$$

$$D_5 = (\epsilon\tan\psi)^{-3} (\nu_5 + 6\nu_6\mu) \quad , \text{ and}$$

$$D_6 = (\epsilon\tan\psi)^{-7/2} \nu_6 \quad ; \tag{B-12}$$

or by the convenient binomial coefficient matrix as

$$\begin{bmatrix} D_0\ (\epsilon \tan\psi)^{1/2} \\ D_1\ (\epsilon \tan\psi) \\ D_2\ (\epsilon \tan\psi)^{3/2} \\ D_3\ (\epsilon \tan\psi)^{2} \\ D_4\ (\epsilon \tan\psi)^{5/2} \\ D_5\ (\epsilon \tan\psi)^{3} \\ D_6\ (\epsilon \tan\psi)^{7/2} \end{bmatrix} = \begin{bmatrix} 1, & \mu, & \mu^2, & \mu^3, & \mu^4, & \mu^5, & \mu^6 \\ 0, & 1, & 2\mu, & 3\mu^2, & 4\mu^3, & 5\mu^4, & 6\mu^5 \\ 0, & 0, & 1, & 3\mu, & 6\mu^2, & 10\mu^3, & 15\mu^4 \\ 0, & 0, & 0, & 1, & 4\mu, & 10\mu^2, & 20\mu^3 \\ 0, & 0, & 0, & 0, & 1, & 5\mu, & 15\mu^2 \\ 0, & 0, & 0, & 0, & 0, & 1, & 6\mu \\ 0, & 0, & 0, & 0, & 0, & 0, & 1 \end{bmatrix} \cdot \begin{bmatrix} \nu_0 \\ \nu_1 \\ \nu_2 \\ \nu_3 \\ \nu_4 \\ \nu_5 \\ \nu_6 \end{bmatrix}$$

Then,

$$I = -\, e^{\frac{(\delta \tan\psi - \epsilon\eta)^2}{4\,\epsilon \tan\psi}} \left\{ \frac{\sqrt{\pi}}{16} (8\,D_0 + 4D_2 + 6D_4 + 15D_6)\ \mathrm{erf}\ \omega \right.$$

$$- \frac{1}{2}\, e^{-\omega^2} \left[(D_1 + D_3 + 3D_5) + \left(D_2 + \frac{3}{2}\, D_4 + \frac{15}{4}\, D_6\right) \omega + (D_3 + 2D_5)\omega^2 \right.$$

$$\left. \left. + \left(D_4 + \frac{5}{2}\, D_6\right)\omega^3 + D_5\,\omega^4 + D_6\,\omega^5 \right] \right\} \quad . \qquad \text{(B-13)}$$

The choice of coordinate system (at the center of the given segment) guarantees symmetric integral limits of the variable x*. But it should be remembered that a linear translation of this variable was made, so it cannot be argued, in general, that the even terms in the last expression vanish. If we reintroduce the initial variables we have

$$\omega = \left\{ (x - x^*) - \left[\frac{\delta \tan\psi + \epsilon(y - x \tan\psi)}{2\,\epsilon \tan\psi} \right] \right\} \sqrt{\epsilon \tan\psi} \quad .$$

Thus,

$$\omega|_{x^*=y_0 \tan\psi} = \left\{ x - y_0 \tan\psi - \left[\frac{\delta \tan\psi + \epsilon(y - x \tan\psi)}{2\epsilon \tan\psi} \right] \right\} \sqrt{\epsilon \tan\psi} = \omega_1 \qquad \text{(B-14)}$$

and

$$\omega|_{x^*=-y_0 \tan\psi} = \left\{ x + y_0 \tan\psi - \left[\frac{\delta \tan\psi + \epsilon(y - x \tan\psi)}{2\epsilon \tan\psi} \right] \right\} \sqrt{\epsilon \tan\psi} = \dot{\omega}_2 \qquad \text{(B-15)}$$

Finally abbreviating,

$$E_0 = \frac{\sqrt{\pi}}{16} (8D_0 + 4D_2 + 6D_4 + 15D_6) \quad ,$$

$$E_1 = \frac{1}{2} (D_1 + D_3 + 3D_5) \quad ,$$

$$E_2 = \frac{1}{2} (D_2 + \frac{3}{2} D_4 + \frac{15}{4} D_6) \quad ,$$

$$E_3 = \frac{1}{2} (D_3 + 2D_5) \quad ,$$

$$E_4 = \frac{1}{2} (D_4 + \frac{5}{2} D_6) \quad ,$$

$$E_5 = \frac{1}{2} D_5 \quad , \text{ and}$$

$$E_6 = \frac{1}{2} D_6 \quad .$$

We have

$$I = + e^{-\frac{(\delta \tan\psi - \epsilon\eta)^2}{4\epsilon \tan\psi}} \left\{ e^{-\omega^2} [E_1 + E_2\omega + E_3\omega^2 + E_4\omega^3 + E_5\omega^4 + E_6\omega^5] - E_0 \operatorname{erf}\omega \right\} \Big|_{\omega_2}^{\omega_1} \quad , \qquad \text{(B-16)}$$

so that

$$\chi = \frac{Q}{2}\,\sigma_z(x_0)\,\sigma_y(x_0)\,e^{-\frac{(\delta \tan\psi - \epsilon\eta)^2}{4\epsilon \tan\psi}} \left\{ E_1 \left(e^{-\omega_1^2} - e^{-\omega_2^2}\right) \right.$$

$$+ E_2 \left(\omega_1 e^{-\omega_1^2} - \omega_2 e^{-\omega_2^2}\right) + E_3 \left(\omega_1^2 e^{-\omega_1^2} - \omega_2^2 e^{-\omega_2^2}\right) + E_4 \left(\omega_1^3 e^{-\omega_1^2}\right.$$

$$\left. - \omega_2^3 e^{-\omega_2^2}\right) + E_5 \left(\omega_1^4 e^{-\omega_1^2} - \omega_2^4 e^{-\omega_2^2}\right) + E_6 \left(\omega_1^5 e^{-\omega_1^2} - \omega_2^5 e^{-\omega_2^2}\right)$$

$$\left. - E_0 \left(\text{erf}\,\omega_1 - \text{erf}\,\omega_2\right) \right\} N(t) \qquad \text{(B-17)}$$

It would be very convenient if equation (B-17) could be inverted to yield y as a function of χ, since this would allow noninterpolative plotting of constant χ isopleths. Such an inversion is not a simple matter, however.

REFERENCES

1. Mathis, Joe J., Jr.; and William L. Grohse: A Review of Methods for Predicting Air Pollution Dispersion. National Aeronautics and Space Administration, NASA SP-322.

2. Crank, J.: The Mathematics of Diffusion. Oxford University Press, 1957.

3. Turner, D. Bruce: Workbook of Atmospheric Dispersion Estimates. Department of Health, Education, and Welfare, Public Health Service, Environmental Health Service; PB 191 482, N 71 31626, 1970.

4. Sutton, O. G.: Micrometeorology. McGraw Hill Book Co., New York, 1953.

5. Gradshteyn, I. S.; and Ryzhik, I. M.: Tables of Integrals, Series, and Products. Academic Press, 1965.

6. Domke, Charles J.: Automobile Exhaust Emission Surveillance: A Summary. Prepared for EPA Office of Air and Water Programs, Office of Mobile Source Air Pollution Control. Certification and Surveillance Division, Ann Arbor, Michigan, 48105, May, 1973.

7. Anon. McGraw Hill Encyclopedia of Science and Technology, McGraw Hill Book Co., New York, N.Y., 1971.

8. Anon.: Draft Environmental Impact Statement: Bellefonte Nuclear Plant. vol. I, Tennessee Valley Authority, undated.

9. Caplan, John. D.: Causes and Control of Automobile Emissions. Hearing Report, Hearings Before a Special Subcommittee on Air and Water Pollution, Committee on Public Work, United States Senate, 89th Congress, First Session on S.306, Washington, D.C., 1965.

10. Stephens, J. Brisco; Susko, Michael; Kaufman, John W.; and Hill, C. Kelly: An Analytical Analysis of the Dispersion Predictions for Effluents from the Saturn V and Scout-Algol III Rocket Exhausts. National Aeronautics and Space Administration, NASA TMX-2935, October, 1973.

11. Fosberry, R.A.C.: Engine Exhaust Emissions and Their Control in Vehicle Operations and Testing. Automotive Technology Series, J. G. Giles, Ed., Iliffe Books Ltd., London, 1969.

12. Gröbner, R. and N. Hofreiter.: Integraltafel. Springer-Verlag, 1961.

APPROVAL

DIFFUSION FROM A LINE SOURCE

By Rowland E. Burns

The information in this report has been reviewed for security classification. Review of any information concerning Department of Defense or Atomic Energy Commission programs has been made by the MSFC Security Classification Officer. This report, in its entirety, has been determined to be unclassified.

This document has also been reviewed and approved for technical accuracy.

E. D. GEISSLER
Director, Aero-Astrodynamics Laboratory